

# Compressing Structured Tensor Algebra

MAHDI GHORBANI\*, University of Edinburgh, UK

EMILIEN BAUER\*, University of Edinburgh, UK

TOBIAS GROSSER, University of Cambridge, UK

AMIR SHAIKHHA, University of Edinburgh, UK

Tensor algebra is a crucial component for data-intensive workloads such as machine learning and scientific computing. As the complexity of data grows, scientists often encounter a dilemma between the highly specialized dense tensor algebra and efficient structure-aware algorithms provided by sparse tensor algebra. In this paper, we introduce DASTAC, a framework to propagate the tensors’s captured high-level structure down to low-level code generation by incorporating techniques such as automatic data layout compression, polyhedral analysis, and affine code generation. Our methodology reduces memory footprint by automatically detecting the best data layout, heavily benefits from polyhedral optimizations, leverages further optimizations, and enables parallelization through MLIR. Through extensive experimentation, we show that DASTAC achieves 1 to 2 orders of magnitude speedup over TACO, a state-of-the-art sparse tensor compiler, and StructTensor, a state-of-the-art structured tensor algebra compiler, with a significantly lower memory footprint.

Additional Key Words and Phrases: Sparse Tensors, Compiler Optimization, Barvinok Algorithm, MLIR

## 1 INTRODUCTION

Tensor algebra is a fundamental component in several data-intensive workloads, such as signal processing [De Lathauwer and De Moor 1998; Muti and Bourennane 2007; Nion and Sidiropoulos 2010], machine learning [Sidiropoulos et al. 2017], computer vision [Panagakis et al. 2021], quantum chemistry [Khoromskaia and Khoromskij 2018; Mutlu et al. 2019], and bioinformatics [Terán et al. 2019]. Numerous lines of research have attempted to specialize and enhance the performance of the tensor algebra computations either through hardware level (e.g., tensor accelerators [Gondimalla et al. 2019; Hegde et al. 2019; Jia et al. 2021] and TPUs [Jouppi et al. 2023]), or software level (e.g., tuned tensor kernels [Dongarra et al. 1990; Wang et al. 2014] and compilation based optimizations [Gareev et al. 2018]).

As the complexity of the data grows, scientists often face a trade-off between highly tuned and specialized frameworks provided for dense tensor algebra computation and efficient and flexible algorithms provided for sparse tensor algebra that leverage the sparsity of input tensors. Dense tensor algebra frameworks [Baghdadi et al. 2019; Grosser et al. 2012; Mullapudi et al. 2015; Vasilache et al. 2018] support a rich set of compile-time optimizations such as vectorization, tiling, and parallelization. This is thanks to well-known memory access patterns and efficient utilization of contiguous memory, despite not knowing the actual data.

Computations over structured tensor algebras are at the core of several important workloads. The structure is an expression of static information on the sparsity and redundancy of the tensors. Sparsity information defines the symbolic set of indices of non-zero values (e.g., diagonal) while redundancy defines a symbolic mapping from the set of indices of repetitive elements to their unique equivalent (e.g., symmetric). Structured matrices have many applications in machine learning [Khamis et al. 2020] and deep learning [Kissel and Diepold 2023]. Diagonal structure used in the ACDC layer [Moczulski et al. 2016], tridiagonal weight matrices mentioned by [Dumitras and Kossentini 2000], and structured neural network pruning for large language models [Wang

\*These authors contributed equally to this work

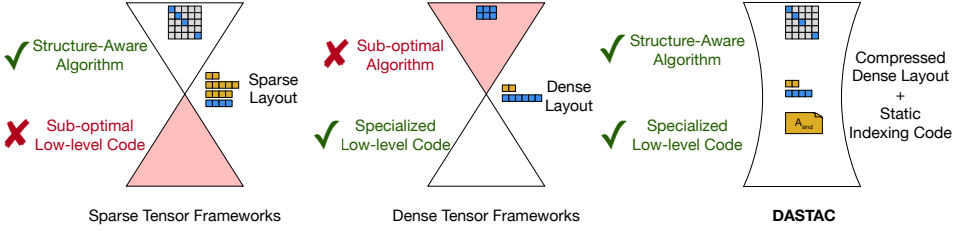


Fig. 1. Comparison of tensor processing frameworks. DASTAC is the first code generation framework that combines the algorithmic optimizations known from sparse tensor algebras with performance-optimized low-level code known from decades of tuning dense tensors.

et al. 2020] are examples of applications of matrices with simple structures. Furthermore, more intricate structures such as hyper triangular for covariance matrices [Ghorbani et al. 2023] and the butterfly structure used for neural network training [Chen et al. 2022] are examples of structured tensor applications.

Sparse tensor algebra frameworks [Chou and Amarasinghe 2022; Ghorbani et al. 2023; Spampinato and Püschel 2016; Virtanen et al. 2020] provide asymptotically improved algorithms by leveraging the sparsity structure of the data with efficient memory storage requirements and better scalability. However, unlike dense counterparts, sparse frameworks cannot leverage the full computation power of the hardware. This is due to irregular data structures, leading to less predictable memory access patterns and making it challenging to fully leverage the same level of optimizations as their dense counterparts.

In this paper, we introduce DASTAC, a framework that propagates the high-level structural information of tensor computations down to the low-level highly tuned code generation (cf. Figure 1). DASTAC leverages a novel symbolic indexing method that compresses an input structured tensor into a densely packed vector representation. In contrast to well-established sparse data layouts like CSR, CSC, or COO, which involve indirect accesses and incur index storage overhead, our method employs efficient direct symbolic index computations. This direct indexing not only diminishes the overall memory footprint but also opens up opportunities for vectorization. These advantages become more important in scenarios where memory bandwidth is the main bottleneck in program efficiency, as is the case on many widespread contemporary hardware, such as CPUs and GPUs.

DASTAC achieves the densely assembled data layout by relying on a well-established mathematical foundation: the polyhedral model. First, DASTAC uses STRUCTENSOR to capture and propagate the structure throughout the tensor algebra computation and then proceeds to apply polyhedral set and map optimizations over the captured structure. Second, DASTAC proceeds to find a densely packed data layout for the tensors involved in the computation and compress them automatically by a novel symbolic indexing algorithm, leading to better cache locality and less memory footprint. Finally, DASTAC generates structure-aware low-level code for CPU using the affine dialect of MLIR [Lattner et al. 2021], enabling effective optimizations at different levels of abstraction. Consequently, DASTAC brings out the best of both dense and sparse tensor algebra worlds together by relying on polyhedral analysis, memory, and complexity efficacy of sparse tensor algebra alongside specialization and compile-time optimization of dense tensor algebra based on polyhedral and compiler optimizations.

Specifically, we make the following contributions:

- We introduce DASTAC, the first framework that integrates the best of both sparse and dense tensor algebra worlds (Section 3). The algorithmic improvements are achieved by leveraging the structure of tensors and this structure is progressively lowered down to the machine-level code.

- DASTAC introduces a densely assembled data layout that enables low-level specialization opportunities (Section 4). The central technique is a novel static indexing algorithm that maps the indices of the input tensor to a contiguous memory buffer.
- We provide a progressive code generation algorithm (Section 5). First, the tensor computations are translated to affine operations provided out-of-the-box by the MLIR framework. Subsequently, at the next stages, the MLIR framework allows DASTAC to benefit from optimizations such as code motion, common subexpression elimination and parallelization.
- We experimentally evaluate DASTAC against state-of-the-art tensor algebra frameworks and show that leveraging structure while benefiting from our proposed compressed data layout and polyhedral optimizations leads to better performance both sequentially and on multi-threaded scenarios (Section 6). We show that DASTAC achieves 1 to 2 orders of magnitude speedup over the TACO sparse tensor compiler and StructTensor, a state-of-the-art structured tensor algebra compiler, with a significantly lower memory footprint. We also show that frameworks such as Polygeist cannot recover the optimizations offered by DASTAC.

## 2 BACKGROUND ON STRUCTURED TENSOR ALGEBRA

Matrices and tensors can have several structures, such as diagonal, tridiagonal, symmetric, and triangular. Leveraging such structures can improve the computational cost of tensor operations by orders of magnitude. For example, leveraging the matrix structure in sparse matrix-vector multiplication (SpMV), where the matrix is diagonal, can lower the computational complexity from  $O(n^2)$  to  $O(n)$ .

Tensor structures can be classified into two categories: 1) sparsity patterns and 2) redundancy patterns. The sparsity patterns refer to structures such as diagonals where zero and non-zero values are distinguished. Structures with redundancy pattern refers to structures such as symmetry, with unique and repetitive elements. The tensor can be reconstructed using the unique values and a mapping from the indices of redundant elements to the unique ones.

STUR [Ghorbani et al. 2023] is the STRUCTTENSOR’s unified intermediate representation used for representing both arithmetic and structural information. STRUCTTENSOR relies on structure inference for tensor computations in the form of unique sets, redundancy maps, and compressed tensors. We explain each component of STUR and how it works using a running example.

**Unique set.** It represents the non-zero and unique (non-repetitive) values of the input tensor and corresponds to capturing the sparsity pattern. For example, the unique set of an  $n \times n$  diagonal matrix  $M$  represented as  $M_U$  is as follows:

$$M_U := \{(x, y) \mid (0 \leq x < n) \wedge (0 \leq y < n) \wedge (x = y)\}$$

Any set representation can be shown in the form of tensor computation over a boolean domain by replacing  $\wedge$  with  $*$  and  $\vee$  with  $+$ . Therefore, the unique set can be represented as follows:

$$M_U(x, y) := (0 \leq x < n) * (0 \leq y < n) * (x = y)$$

**Redundancy map.** It provides the mapping from redundant elements to their corresponding unique elements and corresponds to capturing the redundancy pattern. For example, the unique set and redundancy map for an  $n \times n$  symmetric matrix  $V$  are as follows:

$$\begin{aligned} V_U(x, y) &:= (0 \leq x < n) * (0 \leq y < n) * (x \leq y) \\ V_R(x, y, x', y') &:= (0 \leq x < n) * (0 \leq y < n) * (x > y) * (x' = y) * (y' = x) \end{aligned}$$

Here we are assuming that the lower triangular part of the matrix is the unique part, and the upper triangular part of it is repetitive. Variables  $x, y$  represent the iteration space, and the mapping from the upper triangular to the lower triangular part is represented through variables  $x', y'$ . So this representation means  $x$  and  $y$  values must be swapped to have access to the unique elements.

**Structure inference.** Now imagine the example of sparse matrix-matrix element-wise multiplication where the operands are the aforementioned matrices,  $M$  and  $V$ . To perform this multiplication

while leveraging the structure, STUR applies the program reasoning rules [Ghorbani et al. 2023] to infer this computation’s output structure and compressed iteration space. For the mentioned example, the computation and the inferred output structure after simplification are:

$$\begin{aligned} T(x, y) &:= M(x, y) * V(x, y) \\ T_U(x, y) &:= (0 \leq x < n) * (0 \leq y < n) * (x = y) \\ T_R(x, y, x', y') &:= \emptyset \end{aligned}$$

**Compressed tensor.** It is used for code generation and contains the structural information (the unique set and redundancy map) and the arithmetic operation over tensors using STUR’s syntax. The computation over sets and arithmetic is written using the same intermediate representation (STUR) for structure inference purposes but is treated separately in the code generation process. STRUCTTENSOR internally separates the structural information and arithmetic parts. The structural information is used to generate loops while the arithmetic part generates the computational code inside the loop nests. For example, matrix  $T$  will have the following compressed tensor:

$$T_C(x, y) := (0 \leq x < n) * (0 \leq y < n) * (x = y) * M(x, y) * V(x, y)$$

This means that in this computation, the iterators  $x, y$  should iterate between 0 and  $n$  and must be equal to each other. The arithmetic operation that they perform inside the loop nests is  $M(x, y) * V(x, y)$ . Note that compressed tensor here refers to a tensor that has the structural information, hence, the iteration space can be compressed using this information. The tensor data layout itself is not compressed here. STRUCTTENSOR generates the following code:

```
for (int x = 0; x < n; ++x) {
  int y = x;
  T(x, y) = M(x, y) * V(x, y);
}
```

The first 2 lines are generated by the structural information and the third line is generated because of the arithmetic part of the compressed tensor.

**State-of-the-Art.** STRUCTTENSOR [Ghorbani et al. 2023] introduces the STUR intermediate language with the program reasoning rules to infer structures. As a final step, STRUCTTENSOR provides C++ code that performs the computation over the compressed iteration space. STRUCTTENSOR outperforms sparse and dense tensor algebra competitors by leveraging and propagating the compile-time-known structures throughout the computation.

**Limitations.** Even though STRUCTTENSOR infers the structure, it relies on an uncompressed dense representation of tensors that contains zero and repetitive elements. Alternatively, STRUCTTENSOR requires the user to specify a compact data layout manually, but it is limited to only data layout for inputs. The outputs are still stored in an uncompressed dense format. However, STRUCTTENSOR cannot capture this compressed output data layout. Furthermore, the generated C++ code relies on the low-level compiler (e.g., Clang or GCC) for further optimizations. Thus, one cannot benefit from the more advanced optimizations not supported directly by the compiler (e.g., parallelization).

DASTAC solves both limitations by relying on the mathematical foundation of the polyhedral model. First, it uses a novel symbolic indexing algorithm to densely pack the input and output tensors. Second, benefitting from the progressive lowering between intermediate languages (dialects) provided by the MLIR framework, it applies additional compiler optimizations, including parallelization and vectorization.

### 3 OVERVIEW

In this section, we describe the overall architecture of DASTAC (cf. Figure 2).

**Input.** DASTAC uses STUR as its intermediate language, as it relies on STRUCTTENSOR [Ghorbani et al. 2023] for the structure inference as the first step. STUR can express generalized Einsum

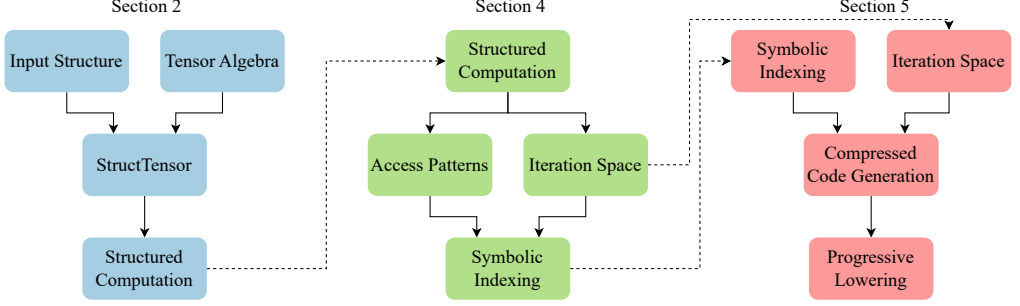


Fig. 2. DASTAC architecture overview.

$$\begin{aligned}
 A(i, j, k) &:= B(i, j, l) * C(k, l) \\
 C_U(k, l) &:= (0 \leq k) * (k < P) * (0 \leq l) * (l < Q) \\
 B_U(i, j, l) &:= (i \leq j) * (0 \leq i) * (i < M) * (0 \leq j) * (j < N) * (0 \leq l) * (l < Q) \\
 A_C(i, j, k) &:= C(k, l) * B(i, j, l) * (0 \leq l) * (Q > l) \\
 &\quad * (i \leq j) * (N > j) * (0 \leq i) * (M > i) * (0 \leq k) * (P > k)
 \end{aligned}$$

Fig. 3. The TTM running example where the first tensor has an upper half cube structure.  $A_C$  represents its optimized structured computation.

expressions as a sum of products (SoP). As an example, Figure 3 shows the STUR representation of the tensor times matrix (TTM) computation with an upper half cube structure.

**Structure inference.** DASTAC proceeds to propagate the input structure throughout the computation by applying program reasoning rules provided by `STRUCTENSOR`. The output structure and compressed computation are inferred during this stage. DASTAC uses the inferred compressed domain by `STRUCTENSOR` as input. For the running example, the output structure is as follows:

$$A_U(i, j, k) := B_U(i, j, l) * C_U(k, l)$$

**Structure Optimizations.** DASTAC improves the structured tensor computation by applying structure optimizations. `STRUCTENSOR` provides a set of optimizations such as inlining and logical simplifications (e.g., set idempotence and addition/multiplication identity optimizations) on the output structure and compressed computation. A polyhedral tool such as `isl` [Verdoolaege 2010] can easily support and apply the aforementioned optimizations alongside further polyhedral set optimizations. Therefore, relying on polyhedral tools can reduce the development cost while increasing the robustness. For these reasons, DASTAC relies on `isl` for further structure optimizations. Figure 3 shows the structured computation for the running example after applying structure optimizations.

**Data Layout Compression.** DASTAC leverages the statically known sparsity structure to assemble a densely packed buffer, aiming for cache-friendliness and vectorization opportunities. Our compression technique consists of a symbolic indexing function, mapping each original tensor index to a linear index of unique and non-zero values. For example, the inferred compressed index of  $B$  in our running example Figure 3 is:

$$P_B(i, j, l) = \left( \left( \left( -\frac{1}{2} + N \right) Q \cdot i - \frac{1}{2} \cdot Q \cdot i^2 \right) + Q \cdot j \right) + l$$

In this expression, the division operator is rational,  $Q$  and  $N$  correspond to the dimensions in Figure 3. Compression and decompression can then be achieved by iterating over the accessed indices and copying the data in and out of the compressed buffer.

```

1  scf.parallel (%arg7) = (%c0) to (%7)
2      step (%c1) {
3      %8 = muli %arg7, %c-1 : index
4      %9 = muli %8, %arg6 : index
5      %10 = muli %arg7, %c2 : index
6      %11 = muli %10, %arg4 : index
7      %12 = muli %11, %arg6 : index
8      %13 = addi %9, %12 : index
9      %14 = muli %arg7, %arg7 : index
10     %15 = muli %14, %c-1 : index
11     %16 = muli %15, %arg6 : index
12     %17 = addi %13, %16 : index
13     %18 = muli %8, %arg3 : index
14     %19 = muli %10, %arg3 : index
15     %20 = muli %19, %arg4 : index
16     %21 = addi %18, %20 : index
17     %22 = muli %15, %arg3 : index
18     %23 = addi %21, %22 : index
19     scf.for %arg8 = %arg7 to %arg4 step %c1 {
20         %24 = muli %arg8, %c2 : index
21         %25 = muli %24, %arg6 : index
22         %26 = addi %17, %25 : index
23         %27 = muli %24, %arg3 : index
24         %28 = addi %23, %27 : index
25         scf.for %arg9 = %c0 to %arg6 step %c1 {
26             %29 = muli %arg9, %c2 : index
27             %30 = addi %26, %29 : index
28             %31 = divui %30, %c2 : index
29             %32 = muli %arg9, %arg3 : index
30             scf.for %arg10 = %c0 to %arg3 step %c1 {
31                 %33 = load %alloc[%31] : memref<?xf64>
32                 %34 = addi %32, %arg10 : index
33                 %35 = load %alloc_0[%34] : memref<?xf64>
34                 %36 = muli %arg10, %c2 : index
35                 %37 = addi %28, %36 : index
36                 %38 = divui %37, %c2 : index
37                 %39 = load %alloc_1[%38] : memref<?xf64>
38                 %40 = mulf %35, %39 fastmath<fast> : f64
39                 %41 = addf %33, %40 fastmath<fast> : f64
40                 store %41, %alloc[%31] : memref<?xf64>
41             }}}}

```

Fig. 4. The compressed kernel code only consists of cheap arithmetic operations, loops, and loads and stores on data. In particular, no index and offset values are loaded from memory such that all memory bandwidth is available for the actual compute workload

**Progressive Code Generation.** DASTAC then proceeds to code generation. It leverages isl’s Abstract Syntax Tree (AST) generation feature, taking a union of iteration domains and optional validity dependencies and returns an AST enforcing those conditions. This AST is then used to generate code in the Affine dialect, a polyhedral-based intermediate representation defined in the MLIR framework. We drive the compilation from this IR down to executable code through MLIR’s provided passes to generate low-level code implementing the used affine operations, simplify the polynomials computation and hoist each part as high as possible in the loop nest, and parallelize the computation by mapping to OpenMP runtime calls. Finally, the resulting LLVM IR is passed to Clang, which provides auto-vectorization and profits from the new opportunities to do so offered by this densely packed data layout representation.

## 4 DATA LAYOUT COMPRESSION

In this section, we present our method for data layout compression using a novel symbolic indexing algorithm, enabling a densely packed representation of the structured sparse tensor elements. This method relies on a symbolic and linear indexing of the values used in a computation. As opposed to well-established sparse data layouts, such as CSR, CSC, or COO, that incur access indirections and index storage overhead, our method uses direct symbolic index computations. This direct indexing simultaneously reduces the global memory footprint and opens vectorization opportunities, two excellent properties when memory bandwidth is a significant constraint on the program efficiency, as is the case on many widespread contemporary hardware, such as CPUs and GPUs.

DASTAC starts the compression process from a tensor computation expressed in STUR (e.g., Figure 3). DASTAC restricts itself to the STUR rules expressed with quasi-affine expressions (affine expressions augmented with modulus). This enables the implementation to leverage mature tools to infer this compressed indexing efficiently.



**Algorithm 1** Symbolic Indexing Algorithm

---

```

1: function SYMBOLICINDEXING( $\mathcal{D}_p, T$ )
2:    $\mathcal{A}_p \leftarrow \text{ACCESSMAPPING}(\mathcal{D}_p, T)$ 
3:    $\mathcal{B}_{p,i} \leftarrow \text{LOCALORDERING}(\mathcal{A}_p, T)$ 
4:    $T_{index}(i, p) \leftarrow \text{SYMBOLICCOUNT}(\mathcal{B}_{p,i})$ 
5:   return PIECEWISEFUSION( $T_{index}$ )
6: end function

```

---

To sidestep combinatorial complexity, DASTAC only works with individual summands of a rule. Take for example the following rule:

$$O(j) := A(i, j) * (i = 1) * (0 \leq j < N) + A(i, j) * (i = 3) * (0 \leq j < N)$$

DASTAC will first infer linear indices for  $O(j)$  and  $A(i, j)$  over the first region, where  $i = 1$ . Only then does it move on to the  $i = 3$  region. In the second region, with  $i = 3$ , a disjoint region of  $A$  is read from, so a second compressed buffer is inferred for this region. On the other hand, the same region of  $O$  is being written to; DASTAC thus "deduplicates" the compressed buffer by simply reusing the one inferred for the first region.

This design decision avoids compile-time costly generalization of the process and is found to work effectively on many motivated cases. However, in all generality, this yields two limitations. First, some values might be duplicated in different compressed buffers, potentially leading to a suboptimal memory footprint reduction in some specific cases. Second, the output compression is only used when output regions are equal (as in the above example) or disjoint, as any other case would potentially lead to partial results being spread across multiple buffers, requiring further computation overhead to have the right values in each buffer.

**Symbolic Indexing Algorithm.** At this stage, DASTAC uses our symbolic indexing algorithm (Algorithm 1) to infer a compressed indexing function. The algorithm takes two inputs. The first input is  $\mathcal{D}_p$  which is an ordered iteration space, where the parameter  $p$  defines symbols such as dimension information. In other words,  $\mathcal{D}_p$  represents the set of iterator values with which the tensor access  $T$  is used. By ordered we mean a sequential execution of the computation. The second input denoted by  $T$ , is the considered tensor access in the form of a function from an iteration to the indices used in this access. The described process in Algorithm 1 is illustrated using buffer  $A$  of our example in Figure 3.

**Iteration space extraction.** To apply Algorithm 1, we define the iteration space of the summand at hand, taking all comparisons of the considered STUR summand. For our running example in Figure 3, the iteration space is:

$$\mathcal{D}_{Q,N,M,P} := \{(i, j, k, l) \in \mathbb{Z}^4 \mid 0 \leq i < M, i \leq j < N, 0 \leq k < P, 0 \leq l < Q\}$$

Here, symbols correspond to the boundary information of dimensions  $(Q, N, M, P)$ . By restricting STUR to affine expressions, one can observe that this set is a polyhedron by construction.

Because we define the iteration space from a high-level representation, we control the order of the dimensions; we simply order them based on their appearance in the rule, ensuring the first iterators are used to index the output, with the last one of them indexing contiguous elements.

**Access mapping.** For each buffer, we define its access map using the access variables used in the STUR expression. By construction, those are affine maps. The corresponding map for buffer  $B$  in Figure 3 is as follows:

$$a_B(i, j, k, l) = (i, j, l)$$

$$\mathcal{A}_{B, \vec{p}} := a_B(\mathcal{D}_{\vec{p}}) = \{\vec{j} \in \mathbb{Z}^m \mid \exists i \in \mathbb{Z}^n : a_B \cdot \vec{i} = \vec{j}, C \cdot \vec{i} + \vec{c} \geq 0\}$$

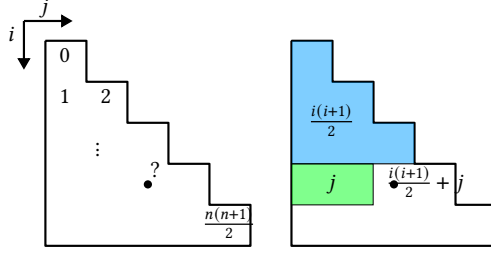


Fig. 5. Illustration of the affine symbolic indexing method, ensuring a dense packing and memory compression.

We apply this mapping on the above iteration space, yielding the set of accessed indices:

$$\mathcal{A}_{Q,N,M,P}^B = a_B(\mathcal{D}_{Q,N,M,P}) = \{(i, j, l) \in \mathbb{Z}^3 \mid 0 \leq i < M, i \leq j < N, 0 \leq l < Q\} \quad (1)$$

**Preceding Accesses.** We proceed to define an order on this accessed domain, using the access map to respect the iteration order. This order is similar to the lexicographic order, only using indices in their iteration domain order. For the map  $a(i, j, k, l) = (k, j, l)$ , this order will be:

$$a(i', j', k', l') < a(i, j, k, l) \iff j' < j \vee j' = j \wedge k' < k \vee j' = j \wedge k' = k \wedge l' < l$$

We use the set of iterators used in the access map in their initial order:

Applying this order to the accessed domain, we define the preceding access domain as the set of all accessed indices preceding a symbolic index. For our running examples, this yields:

$$\begin{aligned} \mathcal{P}_{Q,N,M,P,i,j,l}^B &= \{(i', j', l') \in \mathcal{A}_{Q,N,M,P}^B \mid i' < i\} \\ &\cup \{(i', j', l') \in \mathcal{A}_{Q,N,M,P}^B \mid i' = i \wedge j' < j\} \\ &\cup \{(i', j', l') \in \mathcal{A}_{Q,N,M,P}^B \mid i' = i \wedge j' = j \wedge l' < l\} \end{aligned}$$

**Access domain linearization.** Finally, we can synthesize a mapping from a current iteration to the desired compressed linear index by counting the number of effective accesses preceding this iteration, that is, counting the number of elements of  $\mathcal{A}_{p,i}$ . The Barvinok algorithm [Verdoolaege et al. 5 01] is a method for counting the number of integer points within a parametric polyhedron, returning a piecewise quasi-polynomial (a generalization of polynomials having periodic coefficients) of the polyhedron's parameters.

We can thus use this algorithm, implemented in `isl`, on the preceding access domain and obtain a linear indexing of the accessed domains element, following our chosen order:

$$P_B = \#\mathcal{P}_{p,i}^B$$

**Piecewise Polynomial Simplification.** In general, the counting algorithm yields a *piece-wise* quasi-polynomial, which could have a different expression on distinct subsets of the counted set. In practice, it often yields special cases at boundaries, that are not desirable for simple code generation. For example, when counting the preceding accesses for a triangle as illustrated in Figure 5, the resulting piecewise polynomial is:

$$P = \begin{cases} \frac{1}{2}i + \frac{1}{2}i^2 + j & \text{if } j > 0 \\ \frac{1}{2}i + \frac{1}{2}i^2 & \text{if } j = 0 \end{cases} \quad (2)$$

We apply a piecewise polynomial fusion algorithm presented in Algorithm 2 to simplify the expression of this polynomial. Let us apply this algorithm to our example. We name the two regions as  $D$  and  $D'$ , and their corresponding polynomials as  $P$  and  $P'$ :  $P = \frac{1}{2}i + \frac{1}{2}i^2 + j$ ,  $P' = \frac{1}{2}i + \frac{1}{2}i^2$ . Following line 4 of Algorithm 2, we have  $P - P' = j$ . Restricting this difference to  $D' : j = 0$ , we



**Algorithm 2** Piecewise QuasiPolynomial Fusion Algorithm

---

```

1: function PIECEWISEFUSION( $T_{index}$ )
2:   for all ( $D, P$ ) in  $T_{index}$  do
3:     for all ( $D', P'$ ) in  $T_{index} - (D, P)$  do
4:       if  $(P - P')|_{D'} = 0$  then
5:          $D \leftarrow D \cup D'$ 
6:          $T_{index} \leftarrow T_{index} - (D', P')$ 
7:       end if
8:     end for
9:   end for
10:  return  $T_{index}$ 
11: end function

```

---

```

func.func @plus10(%x : index) -> index {
  %10 = arith.constant 10 : index
  %ret = arith.addi %x, %10 : index
  func.return %ret
}

```

Fig. 6. Example function in MLIR IR.

have  $(P - P')|_{D'} = 0$ ; in other words,  $P$  is equal to  $P'$  on the latter's domain. We thus remove the special case on this domain (line 6), only keeping  $P$  on the union of  $D$  and  $D'$ , yielding a single polynomial expressive enough for the whole buffer:

$$P = \frac{1}{2}i + \frac{1}{2}i^2 + j$$

The computed compressed index for buffer  $A$  in Figure 3 is as follows:

$$P_B(i, j, l) = \left( \left( \left( -\frac{1}{2}Q + Q \cdot N \right) \cdot i - \frac{1}{2}Q \cdot i^2 \right) + Q \cdot j \right) + k$$

In this example, one is expressive enough for the whole buffer; we can thus safely ignore the conditions, knowing by construction we will not index any value out of those bounds.

An interesting side-effect of our design is that the generated piece-wise quasi-polynomials are readily expressed in a form where the slowest varying indices are evaluated the deepest in the expression, making it amenable to effective loop-invariant code hoisting. For example, in  $P_B$ , the most product-intensive term  $(-\frac{1}{2}Q + Q \cdot N)$  can be hoisted of all loops in the computation, as it only depends on the sizes of the tensors.

As our experimental results show, our symbolic indexing algorithm significantly reduces the memory footprint. Furthermore, we observed performance improvements thanks to improved cache locality and enabling vectorization opportunities. Finally, we have not observed significant performance overhead caused by the index computation time on the selected motivated cases.

## 5 PROGRESSIVE CODE GENERATION

Finally, STUR starts generating code using the MLIR framework. It has been chosen as a compiler for this work for its ability to express high-level Intermediate Representation (IR) and lower it progressively to LLVM IR, a low-level IR that the Clang compiler can compile down to binary. This enables MLIR to provide many optimizations at a high level, where the information needed to apply them safely is still present.

```

mark: parallel
iter: i, init: 0, cond: i < min(N,M), inc: 1
  iter: j, init: i, cond: j < N, inc: 1
    iter: k, init: 0, cond: k < P, inc: 1
      iter: l, init: 0, cond: l < Q, inc: 1
        S0[i, j, k, l]
    .
  .
.

→

affine.parallel %i = 0 to min(%N, %M) {
  affine.for %j = %i to %N {
    affine.for %k = 0 to %P {
      affine.for %l = 0 to %Q {
        S0(i, j, k, l);
      }}
  }}

```

Fig. 7. The translation of ISL AST to MLIR’s Affine loops.

## 5.1 MLIR Background

MLIR [Lattner et al. 2021] is a compiler framework successfully applied in the development of compilers in deep learning [Abadi et al. 2015; Paszke et al. 2019], fully-homomorphic encryption [Govindarajan and Moses 2020], and hardware design [Eldridge et al. 2021; Majumder and Bondhugula 2021]. It also opens opportunities, such as compiling our high-level IR down to GPU kernels or other targets rather than generating specialized code and reinventing the wheel, but this has been left as future work.

MLIR IR elementary objects are Operations, Values, Regions, and Attributes. Values represent runtime values and are constrained by the Static Single-Assignment (SSA) form: they can only be assigned once, at definition time. Operations may take values as input and may define new values as output. They can be augmented through attributes, representing various compile-time information. Finally, Operations may contain Regions, which include lists of Operations and possibly entry arguments: Values defined in the region and taking their runtime value from the operation.

An example is given in Figure 6. `func.func` is an Operation representing a function definition. It has a Region representing its body and a function type. In its region, `arith.constant` is an operation only defining a value from a compile-time known value and type. `arith.addi` takes this value and the function’s argument and returns its sum in a new value. Finally, `func.return` only consumes this value to represent returning it from the function.

MLIR implements this idea of mixing levels of abstraction through dialects: collections of operations and types that represent some level of abstraction but can be combined in a program to allow progressive lowering of different parts in a controllable manner. Operations names are prefixed by their dialect’s name: in Figure 6, `arith` and `func` were used.

## 5.2 Affine code generation

**Parallelization.** DASTAC drives ISL to generate an AST expressing parallelism over the outermost index if it is not a reduction. We believe that parallel code generation is a benefit of our densely packed data layout; while similar compaction could be achieved by simple linear indices increments judiciously placed in the loop nest, those would effectively result in loop-carried dependencies, and necessitate further analysis or treatment to parallelize correctly. DASTAC’s symbolic indexing, on the other hand, only depends on current iterators and symbols of the computation; once inferred, it stays a correct mapping however loops are parallelised or further transformed. Thus, parallelism, loop transformations, and compression usage in the generated code become completely orthogonal. Our experiments demonstrate the effectiveness of our compression scheme with simple parallelization (cf. Section 6.2).

**Control Flow Code Generation.** The first step is obtaining an Abstract Syntax Tree (AST) scanning the iteration domain from ISL; an example is in Figure 7. By construction, this AST is guaranteed to have affine bounds and increments. DASTAC uses MLIR’s affine dialect, which expresses affine loops, affine conditions, and affine accesses, to generate IR at the closest abstraction level from its internal one. The main benefit of this approach is that DASTAC does not need to re-implement

```

S0[ $i$ ,
 $j$ ,
 $k$ ,
 $l$ ]
→
%si = affine.apply affine_map<(i,j,k,l)->(i)>(\%i, \%j, \%k, \%l)
%sj = affine.apply affine_map<(i,j,k,l)->(j)>(\%i, \%j, \%k, \%l)
%sk = affine.apply affine_map<(i,j,k,l)->(k)>(\%i, \%j, \%k, \%l)
%sl = affine.apply affine_map<(i,j,k,l)->(l)>(\%i, \%j, \%k, \%l)
%lastval = affine.load %A[%si, %sj, %sl] : memref<?x?xf64>
%factor1 = affine.load %C[%sk, %sl] : memref<?x?xf64>
A(i, j, k) :=
→
%factor2 = affine.load %B[%si, %sj, %sk] : memref<?x?xf64>
C(k, l) * B(i, j, l)
%prod = arith.mulf %factor1, %factor2 : f64
%newval = arith.addf %lastval, %prod : f64
affine.store %A[%si, %sj, %sl] : memref<?x?xf64>

```

Fig. 8. ISL’s schedule is naturally translated to affine maps application and the input computation to accesses and arithmetic.

```

A_C_i = func.call @A_P(%si, %sj, %sl, %Q, %N)
B_C_i = func.call @B_P(%si, %sj, %sk, %Q, %N)
C_C_i = func.call @C_P(%sk, %sl, %N)
A(i, j, k) :=
→
%lastval = memref.load %A_C[%A_C_i] : memref<?x?xf64>
C(k, l) * B(i, j, l)
%factor1 = memref.load %C_C[%C_C_i] : memref<?x?xf64>
%factor2 = memref.load %B_C[%B_C_i] : memref<?x?xf64>
%prod = arith.mulf %factor1, %factor2 : f64
%newval = arith.addf %lastval, %prod : f64
memref.store %A_C[%A_C_i] : memref<?x?xf64>

```

Fig. 9. Using our symbolic indexing, compressed indexing is natural to switch to from dense indexing.

the basics: it simply translates affine expressions from ISL’s to MLIR’s representation and defines loops using those. MLIR is equipped to lower those expressions to arithmetic computations and has advanced infrastructure to simplify those computations at a lower level. Finally, DASTAC generates code corresponding to each statement. For the computation expressed in the STUR language, that means loading each designated value from the right-hand side, multiplying them, and adding that product to the loaded left-hand side value. Memory accesses are translated in two steps to simplify the usage of the compressed indexing polynomial, as explained below.

**Uncompressed Compute Code Generation.** The first step is to apply ISL’s *schedule*, an affine mapping from the current iteration to the values to pass to the statement. In the example given in Figure 4, this schedule is the identity  $\theta(i, j, k, l) = (i, j, k, l)$ .

MLIR’s affine dialect provides an operation to apply a given affine mapping to a list of indices, `affine.apply`, so we use it to define new values corresponding to the scheduled access variables. It then remains to generate the product and accumulation code from the corresponding accesses in the input STUR rule, using MLIR’s basic arithmetic operations. This is all illustrated in Figure 8

**Compressed Compute Code Generation.** Because the inferred compression polynomial is indexing a linear contiguous buffer by directly mapping indices of the original tensor to the corresponding compressed index, generating compressed compute code can be done independently of any control flow; it suffices to generate accesses to the compressed buffers using the inferred polynomial. This is illustrated in Figure 9, where those polynomials are represented as function calls. The attentive reader might notice that we switched from `affine.load` to `memref.load`. Both representing a load operation, the affine variant restricts the access indices to affine expressions of iterators and symbols. Our usage of quasipolynomials breaks this constraint. Here, MLIR’s capacity to mix abstractions is helping because this doesn’t forbid the usage of affine loops and maps where still applicable.

### 5.3 Progressive Lowering

The final step is progressively translating and optimizing this high-level representation to LLVM IR through MLIR. The result of the optimizations is illustrated in Figure 4. The critical steps are as follows (cf. Section 6 for the exact pipeline).

**Function inlining.** The first optimization DASTAC applies is MLIR’s function inlining, `inline`. This is done to expose the quasi-polynomials arithmetic directly in the loop nest, allowing to share computations and hoisting of different parts as high as possible, amortizing their theoretical computational cost.

**Lowering Affine.** The first conversion to execute is from affine operations to arithmetic operations, implementing them through the `lower-affine` pass exposed by MLIR. This will expand all affine map applications, loop bounds, conditions, and accesses to as many basic arithmetic operations as necessary to correctly implement them.

**Generic Optimizations.** CSE is directly applied to the resulting IR. Amongst the different affine and quasipolynomial expressions used in the computation, all expressed on the same iterators and symbols, there are potentially a lot of common sub-expressions. By applying it directly at this level, we allow more opportunities than expecting another lower-level compiler to analyze simplification safety again. The subsequent critical optimization is `canonicalization`, a collection of individual standard optimizations. In this case, we are primarily interested in its constant folding in case any opportunity is open.

**Loop Invariant Code Motion.** Finally, DASTAC uses `loop-invariant-code-motion` to hoist all arithmetic operations as high as possible in the loop nest, leaving only minimal iteration arithmetic in the innermost loop to maximize auto-vectorization opportunities.

## 6 EXPERIMENTAL RESULTS

In this section, we experimentally evaluate our system on a set of application-driven selected kernels. We study the following questions:

- How does DASTAC perform compared to the state-of-the-art tensor algebra frameworks in single- and multi-threaded environments?
- How does the automatic memory compression impact the allocated memory footprint? How do different compression levels improve performance?
- Can DASTAC support complicated structures (e.g., block butterfly factor matrix [Chen et al. 2022])? How does the structure’s complexity impact the compression, run time, and compilation time?
- How does DASTAC scale on various numbers of threads in comparison to state-of-the-art tensor algebra frameworks?
- What is the impact of applying various optimizations compared to the `STRUCTENSOR`? Can state-of-the-art backends (e.g., Polygeist) recover DASTAC’s optimizations?

### 6.1 Experimental Setup

We use a server running Ubuntu 22.04 LTS equipped with a 10-core 2.2 GHz Intel Xeon Silver 4210 CPU with one thread per core and 220 GB of main memory. The server has 32 KB, 1 MB, and 13.8 MB of level 1, 2, and 3 cache, respectively. All C++ code is compiled with Clang 18.0.0 using the following flags:

```
-std=c++17 -O3 -fopenmp -ffast-math -ftree-vectorize -march=native -mtune=native
```

MLIR code is lowered with the pass pipeline:

```
builtin.module(canonicalize, cse, affine-expand-index-ops, lower-affine, finalize-memref-to-llvm,
canonicalize, cse, loop-invariant-code-motion, convert-arith-to-llvm, convert-scf-to-openmp, canonicalize,
```

Table 1. Information on the kernels used for the end-to-end benchmarks.

Kernel	Structure of $B$	Name	Compile Time (s)
<b>TTM</b> $A(i, j, k) := B(i, j, l) * C(k, l)$	Diagonal (plane)	TTM_DP	0.31
	Fixed $j$	TTM_J	0.31
	Upper half cube (UHC)	TTM_UT	0.35
<b>THP</b> $A(i, j, k) := B(i, j, k) * C(i, j, k)$	Diagonal (plane)	THP_DP	0.32
	Fixed $i$	THP_I	0.30
	Fixed $j$	THP_J	0.30
<b>MTTKRP</b> $A(i, j) := B(i, k, l) * C(k, j) * D(l, j)$	Diagonal	MTT_D	0.30
	Fixed $j$ & UHC	MTT_JUT	0.33
	Fixed $j$	MTT_J	0.33
<b>SpMV</b> $A(i) := B(i, j) * C(j)$	Leslie	SpMV_L	0.30
	Upper triangular	SpMV_UT	0.30
	Diagonal	SpMV_D	0.28
<b>Polynomial Regression Degree-D</b> $A^2, \dots, A^{2D}$ where $A^k(i_1, \dots, i_k) := B(x, i_1) * \dots * B(x, i_k)$	Dense, First Dimension Size = 100000	PR2	0.47
	Dense, First Dimension Size = 10000	PR3	1.76
	Dense, First Dimension Size = 2000	PR4	43.18

```
convert-scf-to-cf, convert-func-to-llvm, convert-cf-to-llvm, convert-openmp-to-llvm, reconcile-unrealized-casts)
```

DASTAC does not use tiling, as we did not observe a major benefit (cf. Section 6.6).

As a competitor, we use Polygeist [Moses et al. 2021] to activate out-of-the-box MLIR code generation, polyhedral optimizations (e.g., tiling), and parallelization on top of STRUCTTENSOR, since STRUCTTENSOR lacks such optimizations as it is. Polygeist is shown to have a better single- and multi-threaded performance [Moses et al. 2021] compared to other tools such as Pluto [Bondhugula et al. 2008] and Polly [Grosser et al. 2012]. Polygeist transforms a C code generated based on the inferred structure by STRUCTTENSOR to MLIR with the following lowering pipeline:

```
--canonicalize --cse --affine-expand-index-ops --affine-parallelize --affine-loop-tile --affine-loop-invariant-code-motion --canonicalize --cse --lower-affine --loop-invariant-code-motion --convert-scf-to-openmp --convert-polygeist-to-llvm --canonicalize --cse --loop-invariant-code-motion --canonicalize --cse
```

The lowered code goes through Clang with identical flags to generate executable binary files. For all experiments, the average run time of three runs is reported, as the numbers were stable. All experiments are evaluated using a warm cache. Cache counters are measured using PAPI 7.1 [Laboratory 2023]. As the competitors, we use the latest version of TACO<sup>1</sup> [Kjolstad et al. 2017], NumPy 1.26.0 [Harris et al. 2020], PyTorch 2.0 [Paszke et al. 2019], and TensorFlow 2.14.0 [Abadi et al. 2015] with the XLA backend. All the Python frameworks are run using Python 3.10.13. A dense implementation of the kernels does not leverage any structure and has been shown to perform worse than both sparse and dense tensor algebra frameworks [Ghorbani et al. 2023]; hence, we do not evaluate DASTAC against it.

Table 1 shows kernel information (including the ones used in STRUCTTENSOR [Ghorbani et al. 2023]) with their structure, compilation time (time required for generating MLIR code using DASTAC), and the name we used for them on the plots. This experimental setup has been used previously for STRUCTTENSOR [Ghorbani et al. 2023], a state-of-the-art structured tensor compiler. All the experiments except for the three kernels SpMV\_D, SpMV\_L, and MTT\_D fit in the cache. Table 2 lists the kernels used in our experiments and their input structure representation. For TACO, we picked the best data layout according to the input structure for each kernel (cf. Table 2).

## 6.2 End-to-End Experiments

In this subsection, we evaluated the performance of DASTAC against the best alternative of STRUCTTENSOR (w/ and w/o manual input data layout compression), TACO with the best structure for each kernel, and the best run time of Polygeist applied on the output of STRUCTTENSOR (w/ and

<sup>1</sup><https://github.com/tensor-compiler/taco/tree/2b8ece4c230a5f>

Table 2. Tensor kernels for DASTAC evaluation. In MTT\_J,  $j$  is fixed for  $D$ . In MTT\_D,  $l = j$  too.

Kernel	$B_U$ in STUR	TACO Data Layout
TTM_DP	$(0 \leq i < n_i) * (i = j) * (0 \leq l < n_l)$	$(D, S, D) * (D, D) \rightarrow (D, S, D)$
TTM_J	$(0 \leq i < n_i) * (j = J) * (0 \leq l < n_l)$	$(D, S, D) * (D, D) \rightarrow (D, S, D)$
TTM_UT	$(0 \leq i < n_i) * (i \leq j < n_j) * (0 \leq l < n_l)$	$(D, S, D) * (D, D) \rightarrow (D, S, D)$
THP_DP	$(0 \leq i < n_i) * (i = j) * (0 \leq l < n_l)$	$(D, S, D) * (D, D, D) \rightarrow (D, S, D)$
THP_I	$(i = I) * (0 \leq j < n_j) * (0 \leq l < n_l)$	$(S, D, D) * (D, D, D) \rightarrow (S, D, D)$
THP_J	$(0 \leq i < n_i) * (j = J) * (0 \leq l < n_l)$	$(D, S, D) * (D, D, D) \rightarrow (D, S, D)$
MTT_D	$(i = k = l) * (0 \leq i < n_i)$	$(D, S, S) * (D, D) * (D, S) \rightarrow (D, S)$
MTT_JUT	$(0 \leq i < k) * (0 \leq k < n_k) * (0 \leq l < n_l)$	$(D, S, D) * (D, D) * (D, S) \rightarrow (D, S)$
MTT_J	$(0 \leq i < n_i) * (0 \leq k < n_k) * (0 \leq l < n_l)$	$(D, D, D) * (D, D) * (D, S) \rightarrow (D, S)$
SpMV_L	$(i = 0) * (0 \leq j < n_j) + (1 \leq i < n_i) * (j = i - 1)$	$(D, S) * (D) \rightarrow (D)$
SpMV_UT	$(0 \leq i < n_i) * (i \leq j < n_j)$	$(D, S) * (D) \rightarrow (D)$
SpMV_D	$(0 \leq i < n_i) * (i = j)$	$(D, S) * (D) \rightarrow (D)$

w/o manual input and output data compression, w/ and w/o tiling) on all the kernels (cf. Table 2) in single- and multi-threaded environments.

The number of floating point operations (FLOPs) is computed by multiplying the number of structure-aware iterations for each kernel by the summation of the number of additions and multiplications in that kernel. We used the structure-aware FLOPs since all the systems are leveraging the structure. We set a timeout of ten seconds for all frameworks. All the dense frameworks timed out on all kernels except SpMV with an upper triangular structure and half of TTM with an upper triangular structure. Therefore, we do not include them in any of the figures. The missing points for TACO are due to timeout (for polynomial regression kernels) or segmentation fault because of excessive memory allocation (other kernels). On MTT\_D, all competitors had a segmentation fault (excessive memory allocation) for sizes bigger than 120000.

**Multi-Thread.** Figure 10 compares the performance of each framework’s best version. Static schedule is used for all the experiments. We only show the single-threaded performance results for systems that do not support parallelism (TACO<sup>2</sup> for all kernels except SpMV and STRUCTTENSOR). As shown in Figure 10, DASTAC performs significantly better than all the competitors while running on multi threads. Overall, compared to the competitors, DASTAC can get up to 50× performance enhancement.

In all scenarios, STRUCTTENSOR stands in second place from the performance perspective despite lacking parallelization. This shows the importance of capturing data structure and having an efficient algorithm that leverages this information. TACO’s code cannot be parallelized on any of the kernels, except SpMV, which leads to slower performance. Polygeist automatic parallelization fails to parallelize the code in most cases. The reason behind it is discussed in Section 6.5. In the polynomial regression kernels, TACO times out, Polygeist parallelization descales, and STRUCTTENSOR is running on a single thread; hence, their performance is significantly diminished. DASTAC outperforms them by leveraging the flexibility and efficacy of sparse tensor algebra algorithms and merging them with optimizations and specializations provided by dense tensor algebra through polyhedral techniques. Combined with parallelization, these techniques lead to up to 1 to 2 orders of magnitude performance boost compared to structure-aware competitors.

**Single-Thread.** Figure 11 represents the performance of all frameworks running on a single thread. DASTAC performs on par or outperforms all competitors in almost all cases while running on a single thread. TACO and STRUCTTENSOR achieve closely to DASTAC since they also leverage the structure. However, DASTAC manages to outperform them in most cases (by up to 1 order of magnitude) by having a better memory layout, leading to better cache locality and vectorization.

The downward slope on some kernels (e.g., TTM\_DP and TTM\_J) is due to increased cache miss rate (from 0.2% to 12.6% for TTM\_DP and from 0.2% to 13.2% for TTM\_J) by increasing the

<sup>2</sup>TACO parallelization problem is mentioned in this GitHub issue: The link is removed due to anonymization.



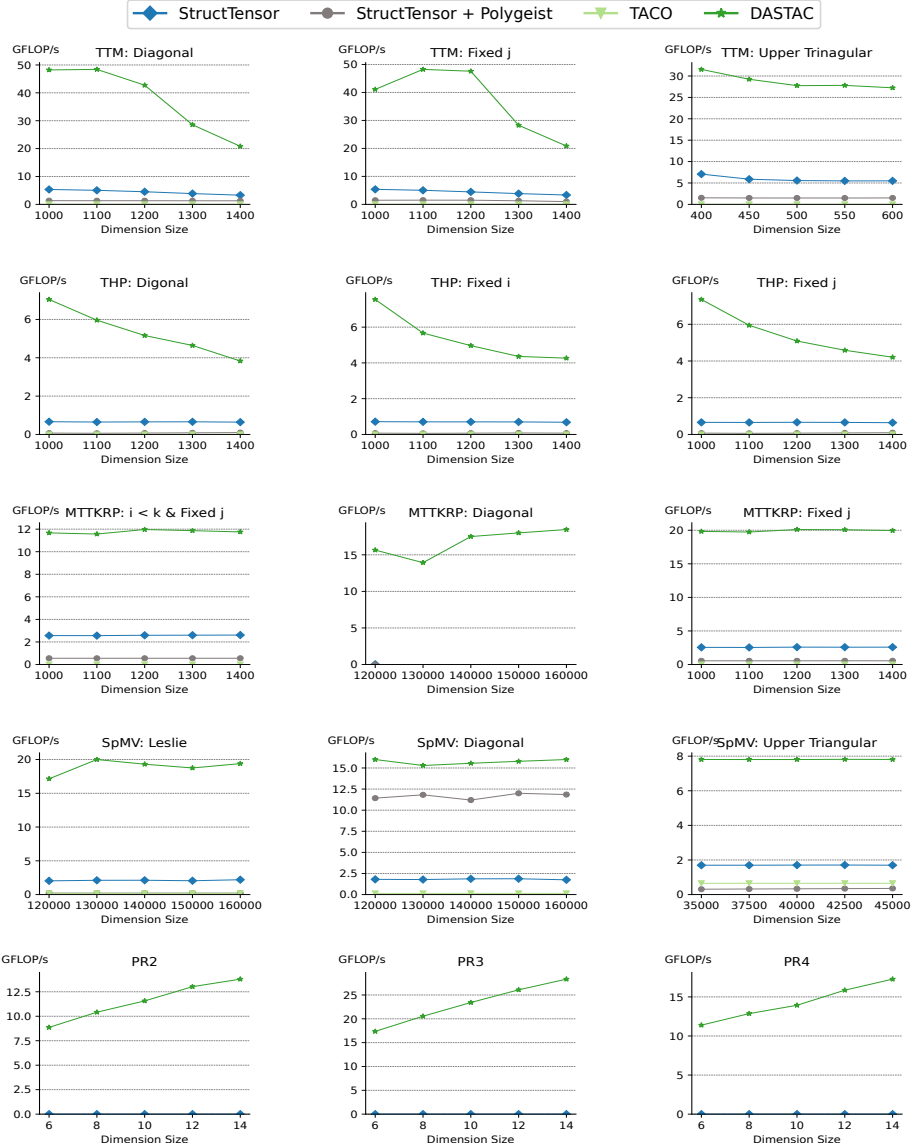


Fig. 10. Performance comparison of various frameworks on ten threads on several structured tensor kernels. In almost all cases, DASTAC shows significantly better performance in comparison with all other competitors.

size (cache miss rate is measured through PAPI for all experiments, but not shown due to space constraints). The generated code by Polygeist fails to outperform DASTAC despite leveraging the structure, manual data layout compression, and having out-of-the-box polyhedral and MLIR optimizations. This shows that using Polygeist to recover affine structure from a lower-level code and applying such optimizations out-of-the-box without a higher-level analysis does not benefit the performance.

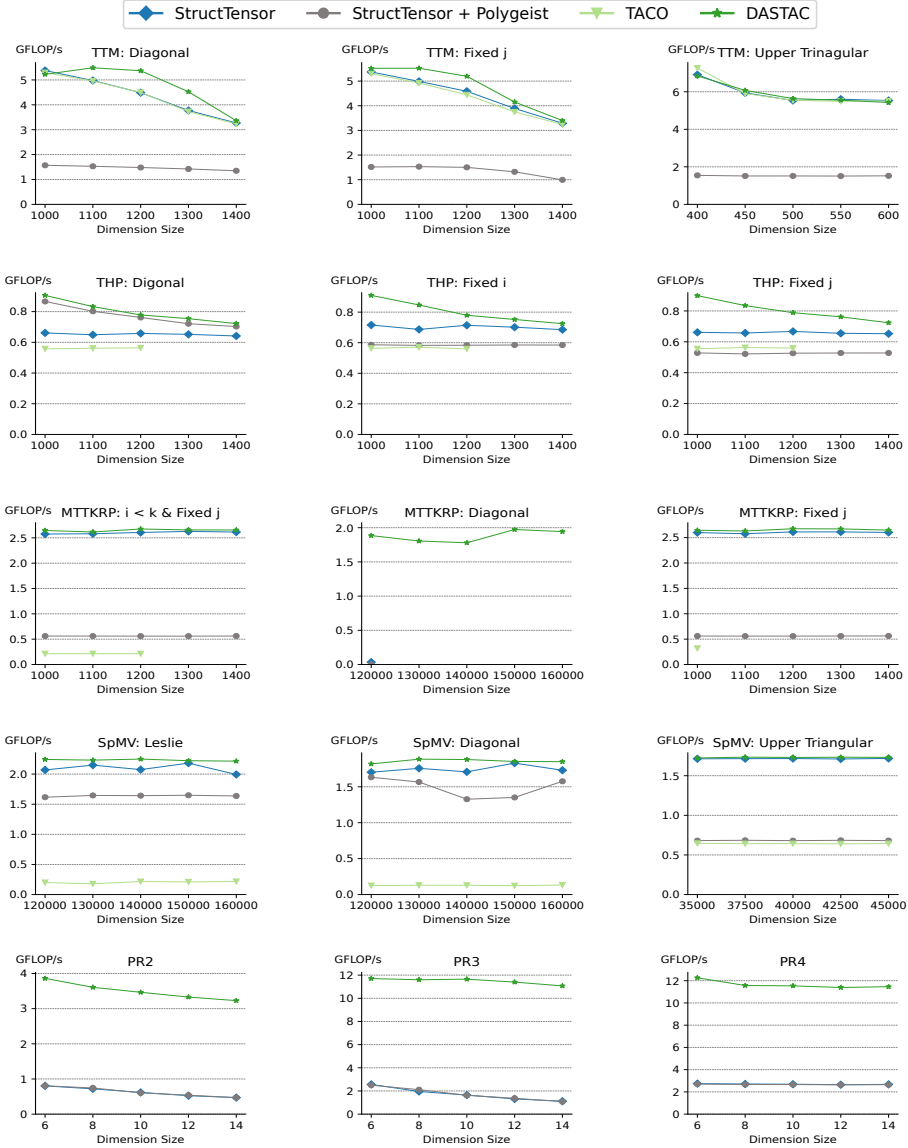


Fig. 11. Performance comparison of various frameworks on one thread on several structured tensor kernels. In all cases, DASTAC performs on par or better than STRUCTTENSOR (w/ and w/o Polygeist).

### 6.3 Memory Compression

**Impact of Compression on Memory Footprint.** We evaluate the impact of the memory compression technique used by DASTAC in comparison to an implementation without compression and STRUCTTENSOR’s manual input compression on six different structures: 1) TTM\_UT, 2) SpMV\_UT, 3) SpMV\_L, 4) TTM\_J, 5) THP\_DP, and 6) MTT\_D (cf. Table 2). We calculate the allocated memory for each structured kernel based on the number of elements allocated for all input and output tensors. The implementation without compression allocates memory for all the elements of the tensors. STRUCTTENSOR reduces the allocated memory to unique elements of the input based on the

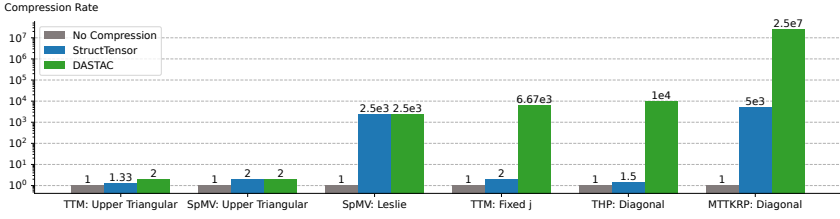


Fig. 12. Evaluation of compression impact on memory footprint of DASTAC and STRUCTTENSOR against an implementation with no compression. The dimension size for all kernels is 10000. DASTAC reaches the maximum compression on all tensors for each kernel, while STRUCTTENSOR often does a sub-optimal job.

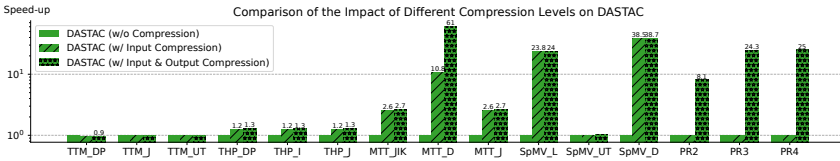


Fig. 13. Evaluation of the impact of different levels of compression on the performance of DASTAC.

structure and all output elements. DASTAC has a better understanding of compression based on the compressed tensor computation and keeps only the elements required for tensor computation in both inputs and output. Therefore, even if a tensor is dense, but some of its elements are not used in the computation, DASTAC compresses the tensor so that unused elements are not stored.

All dimensions for all kernels are considered to be 10000. The compression rate on the y-axis of Figure 12 is the memory allocated by the implementation without compression divided by the memory allocated by other systems. The higher compression rate leads to less memory complexity. Most elements are unique in kernels such as TTM\_UT and SpMV\_UT; therefore, the compression rate is low. Kernels such as SpMV\_UT and SpMV\_L only need the input tensors to be compressed since all the output elements are available and unique; hence, STRUCTTENSOR and DASTAC have the same compression rate. In all other cases, input and output tensors require compression in an ideal scenario. In several kernels, there are unique elements that are not used in the tensor computation (e.g., MTT\_D). Since DASTAC performs computationally structure-aware compression on these kernels, DASTAC’s compression rate is significantly higher than STRUCTTENSOR.

**Impact of Different Levels of Compression.** Figure 13 shows that each level of compression improves the performance for the majority of kernels. Compressing the input has no impact on polynomial regression cases since the input is fully dense. In TTM cases, compression cannot improve the cache locality and the cache miss rate stays the same even after compression, hence, the performance is similar to uncompressed code.

In the tensor computations where the input compression significantly reduces the memory footprint, which leads to a significantly better cache miss rate, output compression has a minimal impact. On the other hand, in tensor expressions where the input is dense or compression over only the input cannot improve the cache accesses significantly, output compression has a larger impact on enhancing the performance.

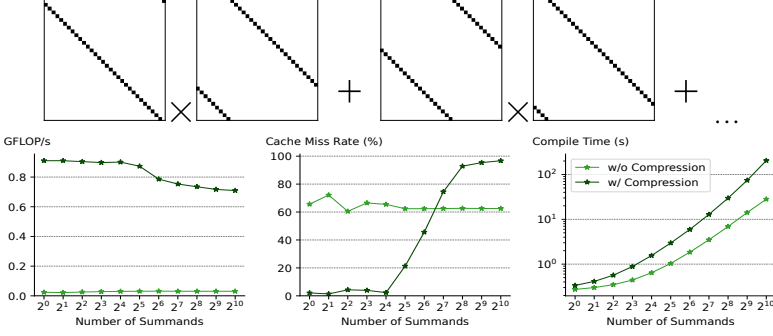


Fig. 14. Evaluation of connection between compression impact and the number of summands using DASTAC. A scaled version of the used structure for this experiment is shown on top.

#### 6.4 Impact of Structure’s Complexity on Compression

In this section, we introduce four new complex structures to study the impact of structure complexity on DASTAC’s compression technique: 1) strided diagonal to study the impact of the number of summands in a tensor operation, 2) block butterfly factor matrix to study the impact of the number of the polyhedrals in the structure, 3) strided band to study the impact of distance of elements, and 4) sub-triangular to study the impact of density.

**Number of Summands in Tensor Computation and Compression.** To measure the connection between these two factors (cf. Figure 14), we consider the following tensor computation:

$$A(i, k) := \sum_{w=1}^p B^w(i, j) * C^w(i, k)$$

where  $B$  and  $C$  have a strided diagonal structure with a random stride. In other words:

$$B_U^w(i, j) := (0 \leq i < N) * (0 \leq j < N) * ((j - i) \% N = s_B^w)$$

The size  $N$  is fixed to  $2^{14}$  here, and the stride  $s_B^w$  is selected randomly for each tensor. The output of each of these multiplications is a strided diagonal with stride  $s_B^w + s_C^w$ . We vary the number of summands from 1 to  $2^{10}$  in powers of 2. More summands result in longer compilation time. Generating code for the compressed version takes longer than without compression since the compression indexing should be computed for more summands. For the compressed version, as the size increases, the number of elements fitting in the cache decreases since the compression cannot compensate anymore; therefore, the cache miss rate goes from almost 0 to almost 100%. The performance starts dropping on the same size that the cache miss rate starts increasing. The generated code without compression has a consistent cache miss rate around 60%, and its performance is also consistently low. This is due to not caching because of high sparsity.

**Number of Polyhedrals and Compression.** To measure the connection between these two factors (cf. Figure 15), we considered a SpMV computation where the matrix dimension is  $2^{14}$  and has a block butterfly factor matrix [Chen et al. 2022]. The structure is as follows:

$$B_U(x, y) := (0 \leq i < b) * (0 \leq j < b) * (0 \leq s < k/2) * (0 \leq c < 2) * (0 \leq d < 2) * (0 \leq r < \frac{n}{k}) * (x = r * k * b + (\frac{c * b * k}{2}) + b * s + i) * (y = r * k * b + (\frac{d * b * k}{2}) + b * s + j)$$

Matrix  $B$  is an  $nb \times nb$  matrix. We set  $n = 2^{10}$  and  $b = 2^4$ . To vary the number of polyhedrals, we unroll this unique set over the variables  $c$ ,  $d$ , and  $s$  and write it as a summation/union format. We also change the value of  $k$  from 2 to  $2^{10}$  in powers of two. This way, the matrix size and density stay exactly the same. However, the underlying structure and the number of polyhedrals change. Therefore, we can measure the impact of changing the number of polyhedrals alone without other factors interfering. The number of polyhedrals is  $2k$ . Increasing the number of polyhedrals increases

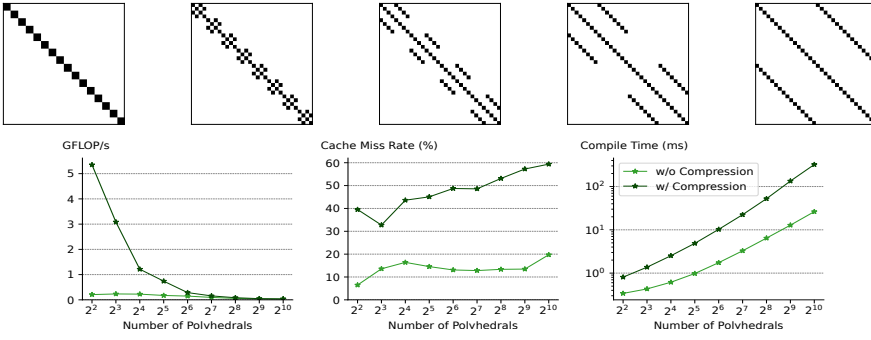


Fig. 15. Evaluation of connection between compression impact and the number of polyhedrals using DASTAC. A scaled version of the used structure for this experiment is shown on top.

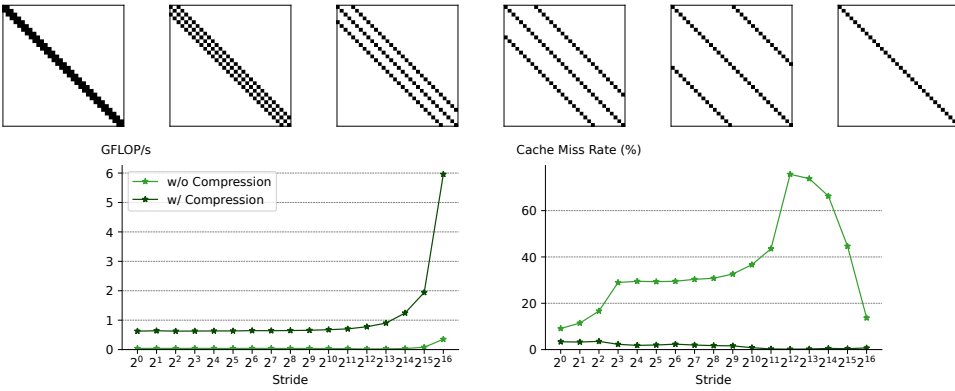


Fig. 16. Evaluation of connection between compression impact and stride of the matrix using DASTAC. A scaled version of the used structure for this experiment is shown on top.

the compilation time for compressed and uncompressed code generation with a similar slope. The cache miss rate for the compressed version increases by increasing the number of polyhedrals since the data is compressed in several buffers rather than fewer contiguous buffers; hence the performance drops. The cache miss rate and performance are consistent for the uncompressed version. The cache miss rate is lower than the compressed version because the iteration space already traverses  $b \times b$  blocks, and compression disrupts the contiguous nature of the buffer.

**Distance of Elements and Compression.** To measure the connection between these two factors (cf. Figure 16), we considered a SpMV computation where the matrix dimension is  $2^{16}$  and has a strided band matrix structure. The structure is as follows:

$$B_U(i, j) := (0 \leq i < N) * (j = i) + (0 \leq i < N) * (j - i = s) + (0 \leq i < N) * (i - j = s)$$

We vary the stride  $s$  from 1 (tridiagonal) to  $2^{16}$  (diagonal). By increasing  $s$ , the number of elements is reduced but their distance is increased. The compressed version mostly fits in the cache and is only impacted by the number of elements. The fewer the elements, the higher the performance and the lower the cache miss rate for the compressed version. The uncompressed version's cache miss rate increases as the distance of the elements increases. However, when the distance reaches beyond  $2^{12}$ , the impact of the decrease in the number of elements helps the cache miss rate to drop. Both versions reach maximum performance when the matrix is diagonal.

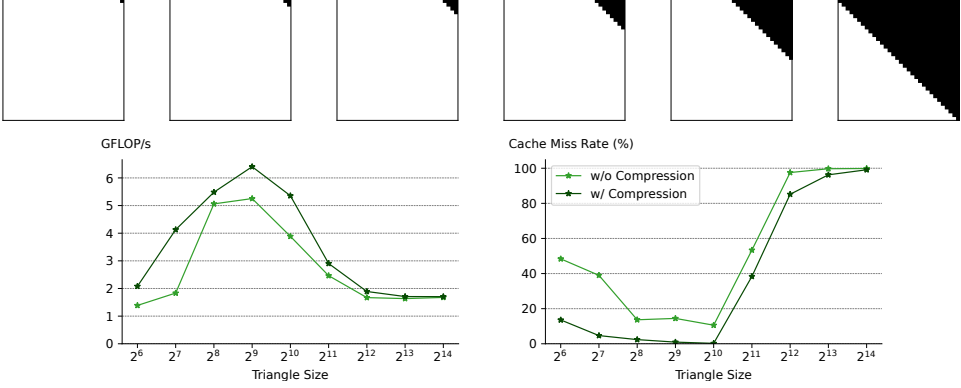


Fig. 17. Evaluation of connection between compression impact and the density of the matrix using DASTAC. A scaled version of the used structure for this experiment is shown on top.

**Density and Compression.** To measure the connection between these two factors (cf. Figure 17), we considered a SpMV computation where the matrix dimension is  $2^{14}$  and has a sub-triangular structure, meaning that the shape is triangular but only contains a subset of an upper triangular matrix. The structure is as follows:

$$B_U(i, j) := (0 \leq i < N) * (0 \leq j < N) * (j - i \geq N - k)$$

Here,  $k$  is the size of the triangle. We vary  $k$  from  $2^6$  to  $2^{14}$  in powers of two. Up to  $k = 2^9$ , the density is low enough to keep all the elements in the cache for the compressed version. Both cases have their best performance on  $k = 2^9$ . After that point, the density and number of elements become larger, hence the compression technique starts losing its benefit compared to uncompressed code. They finally merge into the same cache miss rate and the same performance when the matrix is upper triangular ( $k = 2^{14}$ ).

## 6.5 Parallelization Scalability

We evaluate the DASTAC’s ability to scale on all kernels mentioned in Table 2 by varying the number of threads from one to ten (cf. Figure 18). A considerably large size is selected for all kernels to ensure that the frameworks do not timeout or generate errors (e.g., segmentation fault). The scaling factor on the y-axis shows the speed-up of each framework compared to running them sequentially. As shown in Figure 18, DASTAC can scale almost linearly in most cases by increasing the number of threads. In nearly all cases, DASTAC scales on par or better than state-of-the-art tensor algebra frameworks. In several THP, MTTKRP, and SpMV kernels, DASTAC reaches an almost linear speed-up compared to running it on one thread. TACO only parallelizes on SpMV kernels. STRUCTTENSOR and All other kernels of TACO can not be run in parallel; therefore, they do not scale by varying the number of threads. Only DASTAC can consistently scale up on all kernels. PyTorch fails to scale on polynomial regression kernels, NumPy fails to scale on THP kernels, and TensorFlow fails to scale on SpMV\_UT and SpMV\_D. Polygeist does not scale or even de-scales on the majority of kernels. The automatic parallelization provided by Polygeist leads to parallelizing inner loops and not the outer loops on a majority of kernels. This increases overhead while running on more threads, which leads to a decrease in performance. Furthermore, the code generated by Polygeist for SpMV\_D kernel shows an abnormal behavior on the lower number of threads, which appeared on a range of sizes.



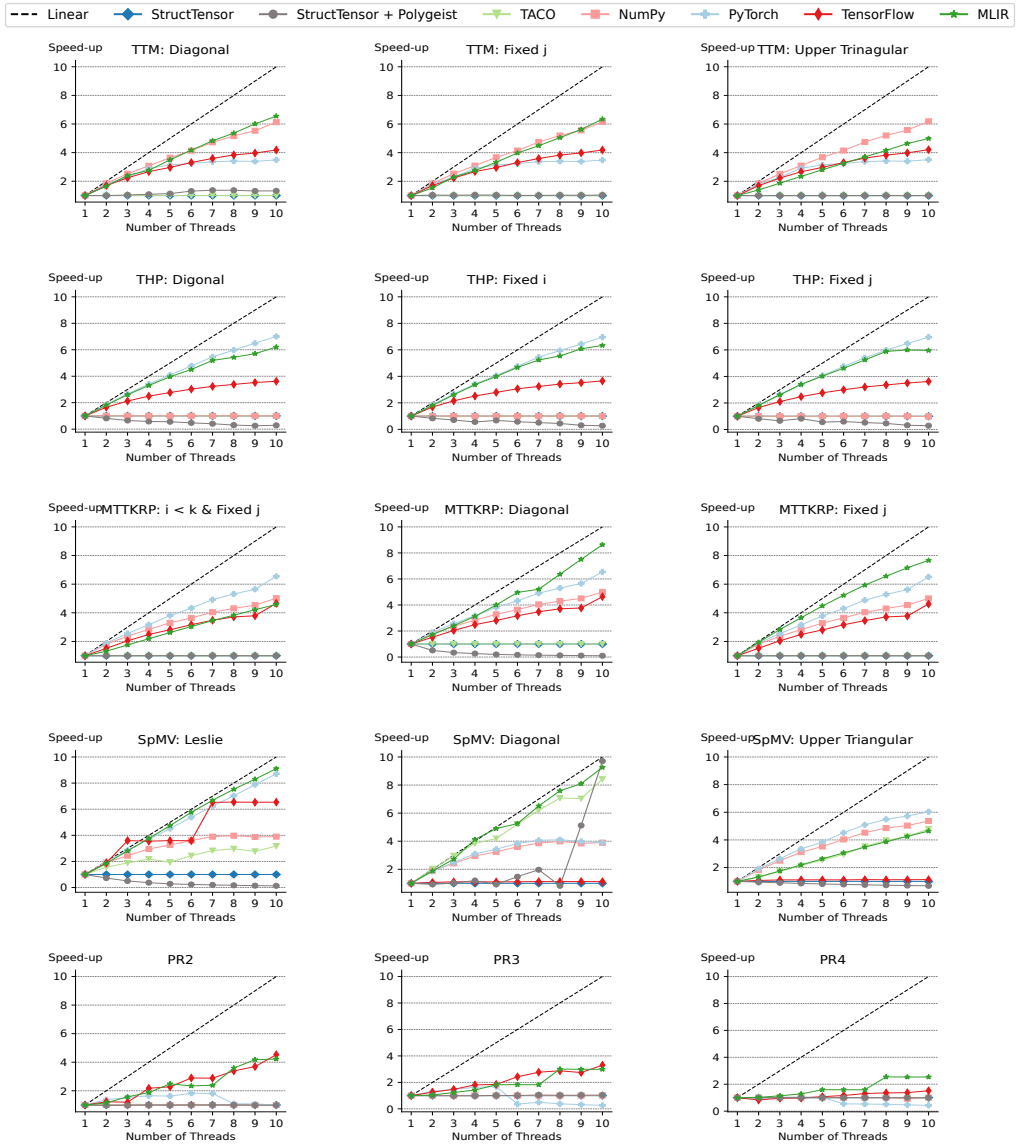


Fig. 18. Comparison of the speed-up scaling of various frameworks on different numbers of threads on several structured tensor operation kernels. In almost all cases, DASTAC scales on par or better than the state-of-the-art tensor algebra frameworks.

### 6.6 Polygeist Performance Using the Structure

Figure 19 shows that manually compressing both input and output almost always improves the performance, except for the cases with a hyper triangular structure, where the compression damages locality. Converting the manually compressed code to Polygeist is usually not helpful and in several cases, it causes performance degradation by removing the existing optimization opportunities for

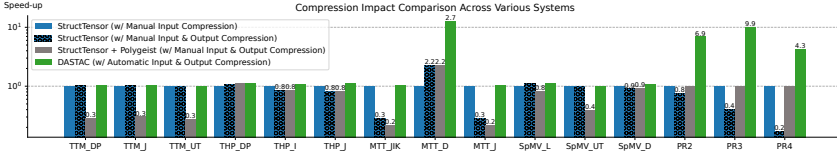


Fig. 19. Evaluation of the impact of different systems’ compression techniques on the performance.

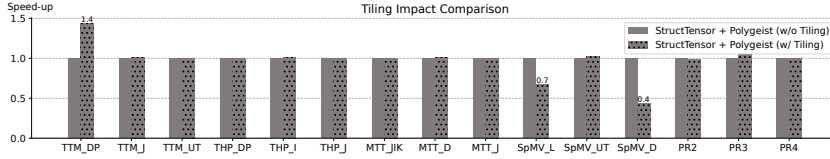


Fig. 20. Evaluation of the impact of Polygeist automatic tiling on the performance.

Clang. DASTAC automatically compresses both input and output based on the iteration space and the compression algorithm almost always enhances the performance over all other competitors.

**Impact of Automatic Tiling Using Polygeist.** Figure 20 shows that out-of-the-box tiling provided by Polygeist does not enhance the performance. Polygeist relies on MLIR compile pass to tile the generated code. However, the out-of-the-box tiling has no impact on the majority of the cases. In cases such as SpMV\_D and SpMV\_L, the iteration space is one-dimensional, and tiling decreases the performance.

## 7 RELATED WORK

In this section, we elaborate on the research that has been done on dense and sparse (unstructured and structured) tensor algebra, as well as data layout compression.

**Dense Tensor Algebra.** Tensor Comprehension [Vasilache et al. 2018] provides optimized code for CUDA kernels by designing a polyhedral-based JIT compiler. TensorFlow [Abadi et al. 2015] and PyTorch [Paszke et al. 2019] are deep learning frameworks providing efficient CPU and GPU code for tensor operation kernels. NumPy [Harris et al. 2020] is a fundamental tool for numerical computing, providing optimized code for dense tensor algebra computations. TVM [Chen et al. 2018] proposes a compiler to address machine learning-specific challenges, making it portable to various hardware devices. All of these systems generate significantly efficient code for dense tensor algebra computations. However, they lack leveraging the structure of the underlying data. isl [Verdoolaege 2010] and CLoog [Bastoul 2004] are generic polyhedral-based frameworks that provide advanced loop optimizations and scheduling and are capable of efficient affine code generation, but they are not full-fledged compiler frameworks and thus lack the ability to densely pack the data layout.

**Unstructured Sparse Tensor Algebra.** The sparse polyhedral framework [Strout et al. 2018] combines the support for sparse tensor algebra with polyhedral techniques. TACO [Chou et al. 2018; Kjolstad et al. 2017] proposes a generic way to handle computation over sparse tensor algebra. SDQL [Schleich et al. 2023; Shaikhha et al. 2024, 2022] uses a functional language to compile sparse tensor programs. JAX [Bradbury et al. 2018] is a high-performance computing tool relying on the MLIR [Lattner et al. 2021] infrastructure with preliminary support for sparse tensor algebra. SciPy [Virtanen et al. 2020] is an algebraic library supporting a variety of kernels supporting both sparse and dense tensor algebra. A DSL to capture sparsity structure for recursive, pointer-based data structures and perform optimized computation on them is provided in [Chou and Amarasinghe

2022]. Recent work on Register Tiling [Wilkinson et al. 2023] relies on low-level optimizations to better exploit compute resources in those cases, but focuses on SpMM only. Those frameworks capture dynamic sparsity nicely. However, they spend extra memory storage to store indexing and go through indirect accesses for computation. DASTAC automatically compresses the tensor data and uses the most efficient data layout. Moreover, DASTAC has direct access to tensor elements by relying on the symbolic polynomial index rather than reading it from an auxiliary array.

Given the interdependencies between the optimal data layout and the target architecture details, recent work has focused on composability [Ye et al. 2023] and interoperability [Bansal et al. 2023] of such transformations to autotune an optimal scheme. These techniques are complementary to our proposed compression technique; exposing symbolic indexing as a composable transformation and augmenting search spaces with its usage is worth exploring in further work.

**Structured Tensor Algebra.** LGen [Spampinato and Püschel 2016] proposes a polyhedral-based algorithm to capture structure on small-scale fixed-size linear algebra computations and generate faster code. EGGs [Tang et al. 2020] unrolls the computation tree to specialize the computation over the sparse data. Sympiler [Cheshmi et al. 2017] performs compile-time symbolic analysis to produce optimized code for a set of linear algebra kernels. A method to capture the unstructured sparsity of matrices in a sparse way to generate polyhedral-based efficient code for the SpMV kernel is proposed in [Augustine et al. 2019]. All the mentioned works are specialized in structured linear algebra and leverage a limited set of operations. However, they are not usable for higher-order tensors and lack a proper automatic data layout compression, and thus are not suitable competitors. STRUCTTENSOR [Ghorbani et al. 2023] captures the structure of tensor algebra computation and propagates it throughout the computation, leading to efficient C++ code generation. However, STRUCTTENSOR’s support for data layout is limited to inputs and requires the user to provide it manually. STRUCTTENSOR does not support an automatic data layout compression despite inferring the structure. Moreover, STRUCTTENSOR does not leverage specialized dense tensor algebra computation and relies on the underlying compiler for optimizations, even though it lowers the problem of structured tensor algebra computation to dense tensor algebra computation. Finch [Ahrens et al. 2024, 2023] supports unstructured and structured sparsity but shares similar limitations. DASTAC supports structured computation over higher-order tensors. Furthermore, DASTAC packs the structured data densely using a symbolic indexing algorithm and enables leveraging polyhedral- and affine-based optimizations.

**Data Layout Compression.** Tiramisu [Baghdadi et al. 2019] proposes a polyhedral compiler producing efficient and portable sparse tensor algebra code by introducing several optimizations, including a hardware-specific data layout transformation on both CPU and GPU. Polyhedral-based techniques to infer a data layout transformation with a better locality suitable for stencil computation over dense tensor algebra are provided in [Henretty et al. 2013]. PolyMage [Mullapudi et al. 2015] utilizes polyhedral techniques to transform the data layout of intermediate computation results and generates affine code for it. All the aforementioned frameworks propose and utilize advanced data layout transformation techniques for enhancing the data locality most suitably for the underlying hardware or based on the computation graph. However, they are only permuting the data without compressing based on the structure of the data. DASTAC automatically infers a data transformation to densely pack the sparse data and provides a compressed data layout for the input, intermediate, and output data. A method using the Barvinok counting algorithm [Verdoolaege et al. 2015] to index iterations in a parallel loop nest to collapse them for coarser parallelism through OpenMP is proposed in [Clauss et al. 2017]. However, this approach does not compress the data and is much more costly compared to DASTAC since it computes the inverse of a quasi-polynomial.

## 8 CONCLUSION

In this paper, we introduce DASTAC, the first code generation framework combining algorithmic optimizations known from sparse tensor algebra frameworks with performance-optimized low-level code known from decades of tuning dense tensors. The central design behind DASTAC is a novel symbolic indexing algorithm to compress the structured tensor data into a contiguous memory buffer. This algorithm relies on the well-established mathematical foundation of polyhedral models, enabling additional optimizations such as optimal conditional placements and parallelization. Our experimental results show that the compressed data layout by DASTAC achieves state-of-the-art memory consumption and sequential/parallel execution run time. In the future, we plan to target architectures such as GPU with applications such as sparse neural networks that can benefit from our proposed algorithm for densely packing tensor data. We also plan to consider other structured data including graphs.

## ACKNOWLEDGEMENT

This work was supported by the Engineering and Physical Sciences Research Council (EPSRC) grant EP/W007940/1 and partly funded by a gift from RelationalAI. The authors thank Huawei for their support of the distributed data management and processing laboratory at the University of Edinburgh.

## REFERENCES

- Martín Abadi, Ashish Agarwal, Paul Barham, Eugene Brevdo, Zhifeng Chen, Craig Citro, Greg S. Corrado, Andy Davis, Jeffrey Dean, Matthieu Devin, Sanjay Ghemawat, Ian Goodfellow, Andrew Harp, Geoffrey Irving, Michael Isard, Yangqing Jia, Rafal Jozefowicz, Lukasz Kaiser, Manjunath Kudlur, Josh Levenberg, Dandelion Mané, Rajat Monga, Sherry Moore, Derek Murray, Chris Olah, Mike Schuster, Jonathon Shlens, Benoit Steiner, Ilya Sutskever, Kunal Talwar, Paul Tucker, Vincent Vanhoucke, Vijay Vasudevan, Fernanda Viégas, Oriol Vinyals, Pete Warden, Martin Wattenberg, Martin Wicke, Yuan Yu, and Xiaoqiang Zheng. 2015. TensorFlow: Large-Scale Machine Learning on Heterogeneous Systems. <https://www.tensorflow.org/> Software available from tensorflow.org.
- Willow Ahrens, Teodoro Fields Collin, Radha Patel, Kyle Deeds, Changwan Hong, and Saman P. Amarasinghe. 2024. Finch: Sparse and Structured Array Programming with Control Flow. *CoRR* abs/2404.16730 (2024). <https://doi.org/10.48550/ARXIV.2404.16730> arXiv:2404.16730
- Willow Ahrens, Daniel Donenfeld, Fredrik Kjolstad, and Saman P. Amarasinghe. 2023. Looplets: A Language for Structured Coiteration. In *Proceedings of the 21st ACM/IEEE International Symposium on Code Generation and Optimization, CGO 2023, Montréal, QC, Canada, 25 February 2023- 1 March 2023*, Christophe Dubach, Derek Bruening, and Ben Hardekopf (Eds.). ACM, 41–54. <https://doi.org/10.1145/3579990.3580020>
- Travis Augustine, Janarthanan Sarma, Louis-Noël Pouchet, and Gabriel Rodriguez. 2019. Generating piecewise-regular code from irregular structures. In *Proceedings of the 40th ACM SIGPLAN Conference on Programming Language Design and Implementation, PLDI 2019, Phoenix, AZ, USA, June 22–26, 2019*, Kathryn S. McKinley and Kathleen Fisher (Eds.). ACM, 625–639. <https://doi.org/10.1145/3314221.3314615>
- Riyadh Baghdadi, Jessica Ray, Malek Ben Romdhane, Emanuele Del Sozzo, Abdurrahman Akkas, Yunming Zhang, Patricia Suriana, Shoaib Kamil, and Saman Amarasinghe. 2019. Tiramisu: A polyhedral compiler for expressing fast and portable code. In *2019 IEEE/ACM International Symposium on Code Generation and Optimization (CGO)*. IEEE, 193–205.
- Manya Bansal, Olivia Hsu, Kunle Olukotun, and Fredrik Kjolstad. 2023. Mosaic: An Interoperable Compiler for Tensor Algebra. *Proc. ACM Program. Lang.* 7, PLDI, Article 122 (jun 2023), 26 pages. <https://doi.org/10.1145/3591236>
- Cédric Bastoul. 2004. Code Generation in the Polyhedral Model Is Easier Than You Think. In *13th International Conference on Parallel Architectures and Compilation Techniques (PACT 2004), 29 September - 3 October 2004, Antibes Juan-les-Pins, France*. IEEE Computer Society, 7–16. <https://doi.org/10.1109/PACT.2004.10018>
- Uday Bondhugula, Albert Hartono, J Ramanujam, and P Sadayappan. 2008. Pluto: A practical and fully automatic polyhedral program optimization system. In *Proceedings of the ACM SIGPLAN 2008 Conference on Programming Language Design and Implementation (PLDI 08), Tucson, AZ (June 2008)*. Citeseer.
- James Bradbury, Roy Frostig, Peter Hawkins, Matthew James Johnson, Chris Leary, Dougal Maclaurin, George Necula, Adam Paszke, Jake VanderPlas, Skye Wanderman-Milne, and Qiao Zhang. 2018. *JAX: composable transformations of Python+NumPy programs*. <http://github.com/google/jax>

- Beidi Chen, Tri Dao, Kaizhao Liang, Jiaming Yang, Zhao Song, Atri Rudra, and Christopher Ré. 2022. Pixelated Butterfly: Simple and Efficient Sparse training for Neural Network Models. In *The Tenth International Conference on Learning Representations, ICLR 2022, Virtual Event, April 25-29, 2022*. OpenReview.net. <https://openreview.net/forum?id=Nfl-iXa-y7R>
- Tianqi Chen, Thierry Moreau, Ziheng Jiang, Lianmin Zheng, Eddie Yan, Haichen Shen, Meghan Cowan, Leyuan Wang, Yuwei Hu, Luis Ceze, et al. 2018. {TVM}: An automated {End-to-End} optimizing compiler for deep learning. In *13th USENIX Symposium on Operating Systems Design and Implementation (OSDI 18)*. 578–594.
- Kazem Cheshmi, Shoaib Kamil, Michelle Mills Strout, and Maryam Mehri Dehnavi. 2017. Sympiler: Transforming Sparse Matrix Codes by Decoupling Symbolic Analysis. In *Proceedings of the International Conference for High Performance Computing, Networking, Storage and Analysis (Denver, Colorado) (SC '17)*. Association for Computing Machinery, New York, NY, USA, Article 13, 13 pages. <https://doi.org/10.1145/3126908.3126936>
- Stephen Chou and Saman Amarasinghe. 2022. Compilation of dynamic sparse tensor algebra. *Proceedings of the ACM on Programming Languages* 6, OOPSLA2 (2022), 1408–1437.
- Stephen Chou, Fredrik Kjolstad, and Saman P. Amarasinghe. 2018. Format abstraction for sparse tensor algebra compilers. *Proc. ACM Program. Lang.* 2, OOPSLA (2018), 123:1–123:30. <https://doi.org/10.1145/3276493>
- Philippe Clauss, Ervin Altintas, and Matthieu Kuhn. 2017. Automatic collapsing of non-rectangular loops. In *2017 IEEE International Parallel and Distributed Processing Symposium (IPDPS)*. IEEE, 778–787.
- Lieven De Lathauwer and Bart De Moor. 1998. From matrix to tensor: Multilinear algebra and signal processing. In *Institute of mathematics and its applications conference series*, Vol. 67. Citeseer, 1–16.
- J. J. Dongarra, Jeremy Du Croz, Sven Hammarling, and I. S. Duff. 1990. A Set of Level 3 Basic Linear Algebra Subprograms. *ACM Trans. Math. Softw.* 16, 1 (mar 1990), 1–17. <https://doi.org/10.1145/77626.79170>
- Adriana Dumitras and Faouzi Kossentini. 2000. Feedforward neural network design with tridiagonal symmetry constraints. *IEEE Trans. Signal Process.* 48, 5 (2000), 1446–1454. <https://doi.org/10.1109/78.839989>
- Schuyler Eldridge, Prithayan Barua, Aliaksei Chapyzhenka, Adam Izraelevitz, Jack Koenig, Chris Lattner, Andrew Lenharth, George Leontiev, Fabian Schuiki, Ram Sunder, et al. 2021. MLIR as hardware compiler infrastructure. In *Workshop on Open-Source EDA Technology (WOSET)*.
- Roman Gareev, Tobias Grosser, and Michael Kruse. 2018. High-performance generalized tensor operations: A compiler-oriented approach. *ACM Transactions on Architecture and Code Optimization (TACO)* 15, 3 (2018), 1–27.
- Mahdi Ghorbani, Mathieu Huot, Shideh Hashemian, and Amir Shaikhha. 2023. Compiling Structured Tensor Algebra. *Proc. ACM Program. Lang.* 7, OOPSLA2, Article 229 (oct 2023), 30 pages. <https://doi.org/10.1145/3622804>
- Ashish Gondimalla, Noah Chesnut, Mithuna Thottethodi, and TN Vijaykumar. 2019. SparTen: A sparse tensor accelerator for convolutional neural networks. In *Proceedings of the 52nd Annual IEEE/ACM International Symposium on Microarchitecture*. 151–165.
- Sanath Govindarajan and William S. Moses. 2020. SyFER-MLIR: Integrating Fully Homomorphic Encryption Into the MLIR Compiler Framework.
- Tobias Grosser, Armin Größlinger, and Christian Lengauer. 2012. Polly - Performing Polyhedral Optimizations on a Low-Level Intermediate Representation. *Parallel Process. Lett.* 22 (2012). <https://api.semanticscholar.org/CorpusID:18533155>
- Charles R. Harris, K. Jarrod Millman, Stéfan J. van der Walt, Ralf Gommers, Pauli Virtanen, David Cournapeau, Eric Wieser, Julian Taylor, Sebastian Berg, Nathaniel J. Smith, Robert Kern, Matti Picus, Stephan Hoyer, Marten H. van Kerkwijk, Matthew Brett, Allan Haldane, Jaime Fernández del Río, Mark Wiebe, Pearu Peterson, Pierre Gérard-Marchant, Kevin Sheppard, Tyler Reddy, Warren Weckesser, Hameer Abbasi, Christoph Gohlke, and Travis E. Oliphant. 2020. Array programming with NumPy. *Nature* 585, 7825 (Sept. 2020), 357–362. <https://doi.org/10.1038/s41586-020-2649-2>
- Kartik Hegde, Hadi Asghari-Moghaddam, Michael Pellauer, Neal Crago, Aamer Jaleel, Edgar Solomonik, Joel Emer, and Christopher W Fletcher. 2019. Extensor: An accelerator for sparse tensor algebra. In *Proceedings of the 52nd Annual IEEE/ACM International Symposium on Microarchitecture*. 319–333.
- Tom Henretty, Richard Veras, Franz Franchetti, Louis-Noël Pouchet, Jagannathan Ramanujam, and Ponnuswamy Sadayappan. 2013. A stencil compiler for short-vector simd architectures. In *Proceedings of the 27th international ACM conference on International conference on supercomputing*. 13–24.
- Liancheng Jia, Zizhang Luo, Liqiang Lu, and Yun Liang. 2021. Tensorlib: A spatial accelerator generation framework for tensor algebra. In *2021 58th ACM/IEEE Design Automation Conference (DAC)*. IEEE, 865–870.
- Norm Jouppi, George Kurian, Sheng Li, Peter Ma, Rahul Nagarajan, Lifeng Nai, Nishant Patil, Suvinay Subramanian, Andy Swing, Brian Towles, et al. 2023. Tpu v4: An optically reconfigurable supercomputer for machine learning with hardware support for embeddings. In *Proceedings of the 50th Annual International Symposium on Computer Architecture*. 1–14.
- Mahmoud Abo Khamis, Hung Q. Ngo, XuanLong Nguyen, Dan Olteanu, and Maximilian Schleich. 2020. Learning Models over Relational Data Using Sparse Tensors and Functional Dependencies. *ACM Trans. Database Syst.* 45, 2 (2020), 7:1–7:66. <https://doi.org/10.1145/3375661>



- Venera Khoromskaia and Boris N Khoromskij. 2018. *Tensor numerical methods in quantum chemistry*. Walter de Gruyter GmbH & Co KG.
- Matthias Kissel and Klaus Diepold. 2023. Structured Matrices and Their Application in Neural Networks: A Survey. *New Gener. Comput.* 41, 3 (2023), 697–722. <https://doi.org/10.1007/S00354-023-00226-1>
- Fredrik Kjolstad, Shoab Kamil, Stephen Chou, David Lugato, and Saman Amarasinghe. 2017. The Tensor Algebra Compiler. *Proc. ACM Program. Lang.* 1, OOPSLA, Article 77 (Oct. 2017), 29 pages. <https://doi.org/10.1145/3133901>
- Innovative Computing Laboratory. 2023. The Performance Application Programming Interface (PAPI). <https://icl.utk.edu/papi/>
- Chris Lattner, Mehdi Amini, Uday Bondhugula, Albert Cohen, Andy Davis, Jacques Pienaar, River Riddle, Tatiana Shpeisman, Nicolas Vasilache, and Aleksandr Zinenko. 2021. MLIR: Scaling Compiler Infrastructure for Domain Specific Computation. In *2021 IEEE/ACM International Symposium on Code Generation and Optimization (CGO)*. IEEE, 2–14. <https://doi.org/10.1109/CGO51591.2021.9370308>
- Kingshuk Majumder and Uday Bondhugula. 2021. HIR: An mlir-based intermediate representation for hardware accelerator description. *arXiv preprint arXiv:2103.00194* (2021).
- Marcin Moczulski, Misha Denil, Jeremy Appleyard, and Nando de Freitas. 2016. ACDC: A Structured Efficient Linear Layer. In *4th International Conference on Learning Representations, ICLR 2016, San Juan, Puerto Rico, May 2-4, 2016, Conference Track Proceedings*, Yoshua Bengio and Yann LeCun (Eds.). <http://arxiv.org/abs/1511.05946>
- William S. Moses, Lorenzo Chelini, Ruizhe Zhao, and Aleksandr Zinenko. 2021. Polygeist: Raising C to Polyhedral MLIR. In *Proceedings of the ACM International Conference on Parallel Architectures and Compilation Techniques (Virtual Event) (PACT '21)*. Association for Computing Machinery, New York, NY, USA, 12 pages.
- Ravi Teja Mullapudi, Vinay Vasista, and Uday Bondhugula. 2015. Polymage: Automatic optimization for image processing pipelines. *ACM SIGARCH Computer Architecture News* 43, 1 (2015), 429–443.
- Damien Muti and Salah Bourennane. 2007. Survey on tensor signal algebraic filtering. *Signal Processing* 87, 2 (2007), 237–249.
- Erdal Mutlu, Karol Kowalski, and Sriram Krishnamoorthy. 2019. Toward generalized tensor algebra for ab initio quantum chemistry methods. In *Proceedings of the 6th ACM SIGPLAN International Workshop on Libraries, Languages and Compilers for Array Programming*. 46–56.
- Dimitri Nion and Nicholas D Sidiropoulos. 2010. Tensor algebra and multidimensional harmonic retrieval in signal processing for MIMO radar. *IEEE Transactions on Signal Processing* 58, 11 (2010), 5693–5705.
- Yannis Panagakis, Jean Kossaifi, Grigorios G Chrysos, James Oldfield, Mihalis A Nicolaou, Anima Anandkumar, and Stefanos Zafeiriou. 2021. Tensor methods in computer vision and deep learning. *Proc. IEEE* 109, 5 (2021), 863–890.
- Adam Paszke, Sam Gross, Francisco Massa, Adam Lerer, James Bradbury, Gregory Chanan, Trevor Killeen, Zeming Lin, Natalia Gimelshein, Luca Antiga, Alban Desmaison, Andreas Kopf, Edward Yang, Zachary DeVito, Martin Raison, Alykhan Tejani, Sasank Chilamkurthy, Benoit Steiner, Lu Fang, Junjie Bai, and Soumith Chintala. 2019. PyTorch: An Imperative Style, High-Performance Deep Learning Library. In *Advances in Neural Information Processing Systems 32*. Curran Associates, Inc., 8024–8035. <http://papers.neurips.cc/paper/9015-pytorch-an-imperative-style-high-performance-deep-learning-library.pdf>
- Maximilian Schleich, Amir Shaikhha, and Dan Suci. 2023. Optimizing tensor programs on flexible storage. *Proceedings of the ACM on Management of Data* 1, 1 (2023), 1–27.
- Amir Shaikhha, Mathieu Huot, and Shideh Hashemian. 2024. A Tensor Algebra Compiler for Sparse Differentiation. In *IEEE/ACM International Symposium on Code Generation and Optimization, CGO 2024, Edinburgh, United Kingdom, March 2-6, 2024*. Tobias Grosser, Christophe Dubach, Michel Steuwer, Jingling Xue, Guilherme Ottoni, and ernando Magno Quintão Pereira (Eds.). IEEE, 1–12. <https://doi.org/10.1109/CGO57630.2024.10444787>
- Amir Shaikhha, Mathieu Huot, Jaclyn Smith, and Dan Olteanu. 2022. Functional collection programming with semi-ring dictionaries. *Proc. ACM Program. Lang.* 6, OOPSLA1 (2022), 1–33. <https://doi.org/10.1145/3527333>
- Nicholas D Sidiropoulos, Lieven De Lathauwer, Xiao Fu, Kejun Huang, Evangelos E Papalexakis, and Christos Faloutsos. 2017. Tensor decomposition for signal processing and machine learning. *IEEE Transactions on signal processing* 65, 13 (2017), 3551–3582.
- Daniele G. Spampinato and Markus Püschel. 2016. A basic linear algebra compiler for structured matrices. In *Proceedings of the 2016 International Symposium on Code Generation and Optimization, CGO 2016, Barcelona, Spain, March 12-18, 2016*, Björn Franke, Youfeng Wu, and Fabrice Rastello (Eds.). ACM, 117–127. <https://doi.org/10.1145/2854038.2854060>
- Michelle Mills Strout, Mary W. Hall, and Catherine Olschanowsky. 2018. The Sparse Polyhedral Framework: Composing Compiler-Generated Inspector-Executor Code. *Proc. IEEE* 106, 11 (2018), 1921–1934. <https://doi.org/10.1109/JPROC.2018.2857721>
- Xuan Tang, Teseo Schneider, Shoab Kamil, Aurojit Panda, Jinyang Li, and Daniele Panozzo. 2020. EGGs: Sparsity-Specific Code Generation. *Comput. Graph. Forum* 39, 5 (2020), 209–219. <https://doi.org/10.1111/cgf.14080>



- Julio E Terán, Yovani Marrero-Ponce, Ernesto Contreras-Torres, César R García-Jacas, Ricardo Vivas-Reyes, Enrique Terán, and F Javier Torres. 2019. Tensor algebra-based geometrical (3D) biomacro-molecular descriptors for protein research: Theory, applications and comparison with other methods. *Scientific Reports* 9, 1 (2019), 11391.
- Nicolas Vasilache, Oleksandr Zinenko, Theodoros Theodoridis, Priya Goyal, Zachary DeVito, William S. Moses, Sven Verdoolaege, Andrew Adams, and Albert Cohen. 2018. Tensor Comprehensions: Framework-Agnostic High-Performance Machine Learning Abstractions. *CoRR* abs/1802.04730 (2018). arXiv:1802.04730 <http://arxiv.org/abs/1802.04730>
- Sven Verdoolaege. 2010. isl: An Integer Set Library for the Polyhedral Model. In *Mathematical Software – ICMS 2010*, Komei Fukuda, Joris van der Hoeven, Michael Joswig, and Nobuki Takayama (Eds.). Springer Berlin Heidelberg, Berlin, Heidelberg, 299–302.
- Sven Verdoolaege, Rachid Seghir, Kristof Beyls, Vincent Loechner, and Maurice Bruynooghe. 2007-05-01. Counting integer points in parametric polytopes using Barvinok’s rational functions. , 37 - 66 pages.
- Pauli Virtanen, Ralf Gommers, Travis E Oliphant, Matt Haberland, Tyler Reddy, David Cournapeau, Evgeni Burovski, Pearu Peterson, Warren Weckesser, Jonathan Bright, et al. 2020. SciPy 1.0: fundamental algorithms for scientific computing in Python. *Nature methods* 17, 3 (2020), 261–272.
- Endong Wang, Qing Zhang, Bo Shen, Guangyong Zhang, Xiaowei Lu, Qing Wu, Yajuan Wang, Endong Wang, Qing Zhang, Bo Shen, et al. 2014. Intel math kernel library. *High-Performance Computing on the Intel® Xeon Phi™: How to Fully Exploit MIC Architectures* (2014), 167–188.
- Ziheng Wang, Jeremy Wohlwend, and Tao Lei. 2020. Structured Pruning of Large Language Models. In *Proceedings of the 2020 Conference on Empirical Methods in Natural Language Processing, EMNLP 2020, Online, November 16-20, 2020*, Bonnie Webber, Trevor Cohn, Yulan He, and Yang Liu (Eds.). Association for Computational Linguistics, 6151–6162. <https://doi.org/10.18653/V1/2020.EMNLP-MAIN.496>
- Lucas Wilkinson, Kazem Cheshmi, and Maryam Mehri Dehnavi. 2023. Register Tiling for Unstructured Sparsity in Neural Network Inference. *Proc. ACM Program. Lang.* 7, PLDI, Article 188 (jun 2023), 26 pages. <https://doi.org/10.1145/3591302>
- Zihao Ye, Ruihang Lai, Junru Shao, Tianqi Chen, and Luis Ceze. 2023. SparseTIR: Composable Abstractions for Sparse Compilation in Deep Learning. In *Proceedings of the 28th ACM International Conference on Architectural Support for Programming Languages and Operating Systems, Volume 3* (<conf-loc>, <city>Vancouver</city>, <state>BC</state>, <country>Canada</country>, </conf-loc>) (*ASPLOS 2023*). Association for Computing Machinery, New York, NY, USA, 660–678. <https://doi.org/10.1145/3582016.3582047>